



Field trip guide to selected studies of the Southwest Mineral and Environmental Investigations Project in southeastern Arizona.

by B.B. Houser, M.E. Gettings, M.W. Bultman, Floyd Gray,
K.R. Caruthers, and D.M. Hirschberg¹

Open-File Report 99-544

1999

This report is preliminary and has not been reviewed for conformity with U.S. Geological Survey editorial standards. Any use of trade, product, or firm names is for descriptive purposes only and does not imply endorsement by the U.S. Government.

U.S. DEPARTMENT OF THE INTERIOR
U. S. GEOLOGICAL SURVEY

¹ Tucson, AZ



**Field trip guide to selected studies of the
Southwest Mineral and Environmental
Investigations Project in southeastern
Arizona**



**Southwest Field Office
Western Minerals Resources Program
U.S. Geological Survey**

FIELD TRIP GUIDE

An overview of selected areas of study of the Southwest Mineral and Environmental Investigations Project in southeastern Arizona

Contents

Introduction	3
Road log	3
Tucson basin	6
Santa Catalina and Rincon Mountains	6
Empire Mountains	7
Rosemont	7
Whetstone Mountains	8
Greaterville gold placer mining district	8
Kentucky Camp	9
Sonoita	9
STOP 1 -- UPPER SAN PEDRO VALLEY	10
Regional setting	10
Surficial geology and geomorphology	10
Upper San Pedro Valley geophysical studies	12
Canelo Hills	21
STOP 2 -- SAN RAFAEL VALLEY	22
Introduction and geophysical studies	22
STOP 3 -- PATAGONIA CITY PARK	29
Patagonia (town)	29
Patagonia and Santa Rita Mountains	29
Red Mountain overview - volcanic stratigraphy and alteration	30
Mineralization and mining history	32
Overviews of region's hydrologic profile and initial results of SW Mineral and Environmental task 3	35
STOP 4 -- AZTEC GULCH	38
STOP 5 -- SONOITA CREEK AT THE NATURE CONSERVANCY PRESERVE	39
Tumacacori Mountains and Mount Benedict fault	43
STOP 6 -- AEROMAGNETIC SURVEY	43
Santa Cruz Valley and western Santa Rita Mountains	43
References cited	47

Cover photograph: Red Mountain as seen from Aztec Gulch Road, courtesy of Mark Bultman.

List of figures

- Figure 1 Geologic map of southeastern Arizona showing field trip route 4
- Figure 2 Map of part of southeastern Arizona showing field trip route and geographic features mentioned in text 5
- Figure 3 Thematic Mapper image of the upper San Pedro Valley 11
- Figure 4 Locations of airborne electromagnetic flight lines in the upper San Pedro basin 15
- Figure 5 View of conductivity-depth transform cross sections parallel to flight lines 16
- Figure 6 View of conductivity-depth transform cross sections perpendicular to flight lines 16
- Figure 7 View of slice through conductivity-depth transform data cube 16
- Figure 8 Resistivity in test wells 19
- Figure 9 Upper resistivity minimum map 20
- Figure 10 Water-table elevation minus upper resistivity minimum map 20
- Figure 11 Lithologic signatures of magnetic data 24
- Figure 12 Thematic Mapper image of the San Rafael Valley and the Patagonia Mountains 25
- Figure 13 Map of geometry, structure, and concealed geology, San Rafael basin 27
- Figure 14 West to east gravity model profile, San Rafael basin 28
- Figure 15 Precipitation in the Patagonia Mountains 31
- Figure 16 Geohydrologic map of the Red Mountain and Sonoita Creek drainage area 33
- Figure 17 Principal hydrologic units of the southern Basin and Range Province 34
- Figure 18 Plot showing variations in aqueous metal concentrations as a function of pH 36
- Figure 19 Plots of storm flood events showing contaminant influence 41
- Figure 20 Generalized geologic map of the upper Santa Cruz Valley showing location of subbasins 44
- Figure 21 Aeromagnetic map of Mt. Benedict area, upper Santa Cruz Valley, showing the asymmetric graben along the Mt. Benedict fault 45

FIELD TRIP GUIDE

An overview of selected areas of study of the Southwest Mineral and Environmental Investigations Project in southeastern Arizona

by

B.B. Houser, M.E. Gettings, M.W. Bultman,
Floyd Gray, K.R. Caruthers, and D.M. Hirschberg

Introduction

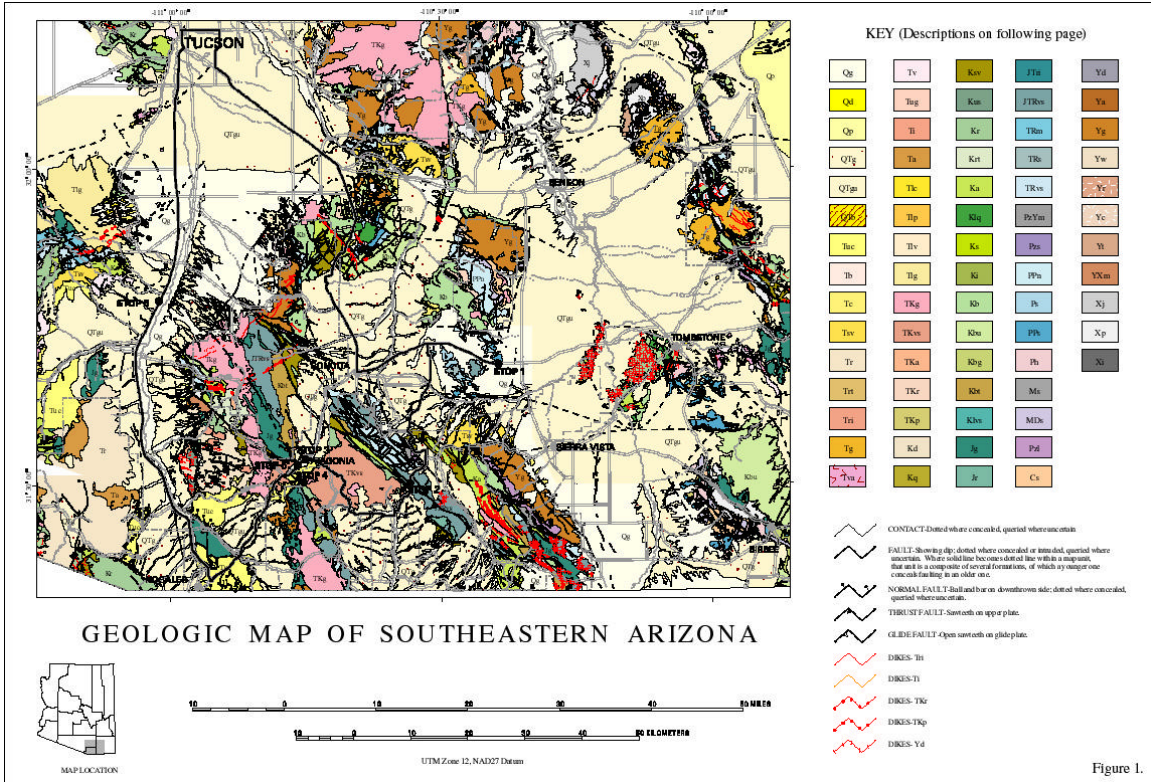
The Southwest Mineral and Environmental Investigations Project is designed to address issues raised by rapid urban development in the basins of the southwestern U.S. These issues require objective geoscientific data that can be used by land managers and stakeholders to develop informed land and water use strategies. The project integrates new and existing geologic, geophysical, and geochemical data, and imagery to provide three-dimensional visualizations of the basins of southeastern Arizona. Emphasis is on developing better knowledge of the aquifer systems of both the basins and the ranges, on acquiring background and baseline information, and on determining the distribution of metals related to mineralization and the fate of these metals in surface and subsurface environments. The products of the project will be used in resolving issues of water quality and quantity, in understanding environmental impacts such as riparian ecosystem maintenance, and in evaluating mineral resources beneath and within the basins.

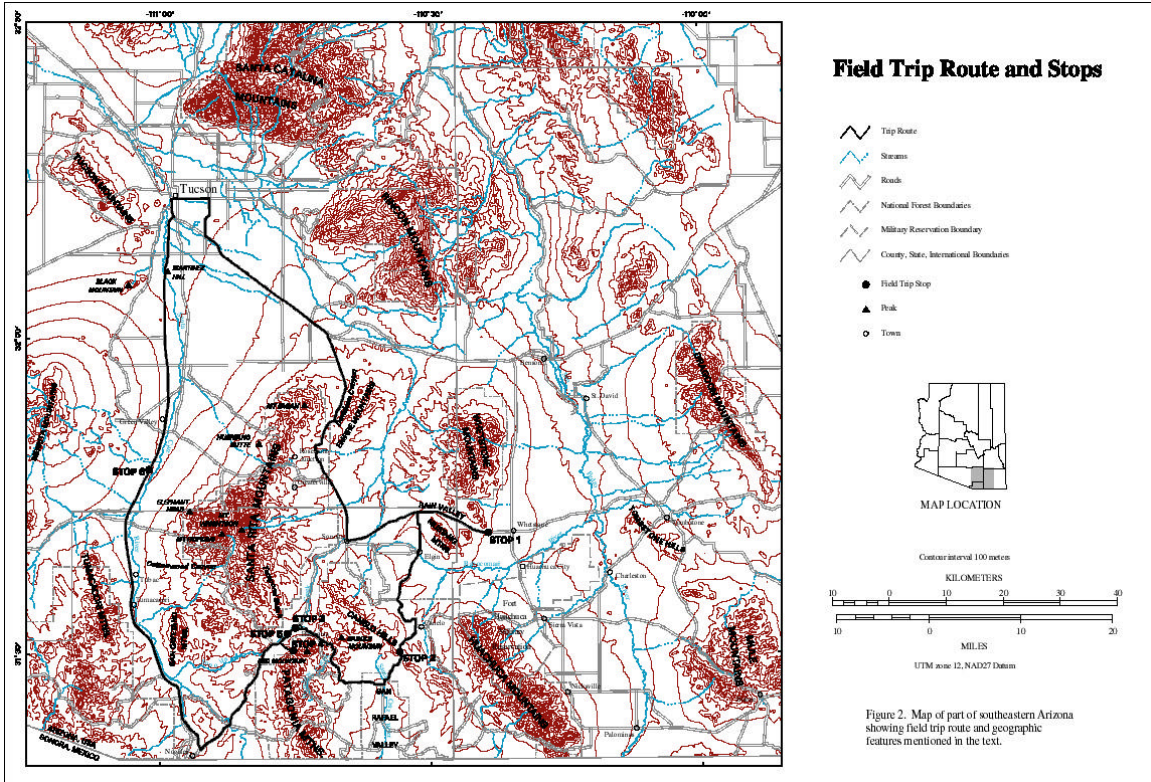
The field trip highlights three topics and areas (figs. 1 and 2): (1) geology and geophysics of the upper San Pedro and upper Santa Cruz basins (M.E. Gettings, M. W. Bultman, and B.B. Houser), (2) geology, geophysics, and mineral resource potential of the San Rafael basin (M.W. Bultman), and (3) hydrology and aqueous geochemistry of the Red Mountain and Sonoita Creek drainage system (Floyd Gray). The trip guide, which begins and ends in Tucson, Arizona, also includes commentary on the cultural and mining history of the area.

Road Log

Mileage

0.0 Depart Environment and Natural Resources Building at East 6th St. and North Park Ave. and proceed to I-10 by way of East 6th St., North Campbell Ave., and Kino Parkway, Tucson, Arizona. See figure 1 for a geologic map showing the trip route and





[Click here to see full view.](#)

location of stops, and figure 2 for a map of physical and cultural features referred to in the text.

4.5 Go east on I-10.

Tucson basin

The Tucson basin (figs. 1 and 2) is a broad irregularly-shaped basin, about 40 km wide and 70 km long, that probably owes its shape to several interacting tectonic elements. It is truncated on the northeast by the Santa Catalina and Rincon Mountains, which comprise the Catalina core complex (Dickinson, 1991). The northwest-trending northern boundary of the Jurassic magmatic arc passes beneath the northern part of the basin, roughly parallel to the Santa Catalinas and Rincons. Cuttings and geophysical logs from a petroleum exploration well (Exxon State (32)-1) drilled near the middle of the basin show the following stratigraphy (Houser and Gettings, 2000):

Pleistocene (?) to middle (?) Miocene
 0-908 - upper basin-fill sedimentary rocks
 908-1,880 - lower basin-fill sedimentary rocks
lower Miocene and upper Oligocene
 1,880-2,516 - Pantano Formation
lower Miocene to Paleocene (?)
 2,516-3,056 - volcanic and sedimentary rocks
Lower Cretaceous to Upper Jurassic
 3,056-3,658 - Bisbee Group
pre-Late Jurassic
 3,658-3,827 - granitoid plutonic rock

Santa Catalina and Rincon Mountains

Drewes (1996) described the Santa Catalina and Rincon Mountains (figs. 1 and 2) as follows: The central parts are underlain by plutonic and metamorphic rocks of Proterozoic, Late Cretaceous, and early to middle Tertiary ages. These crystalline rocks form the cores of the two ranges and are present in the overlying and flanking terranes. Most of the overlying and flanking terranes are underlain by Paleozoic, Mesozoic, and middle Tertiary sedimentary formations and their metasedimentary equivalents. Most crystalline core rocks are foliated and lineated and are protoclastically mylonitized. The foliation and attitudes of the overlying cover rocks are arched into broad gentle domes whose southwestern flanks are folded into southwestward-plunging anticlines and synclines. The lineation is primarily in the plane of foliation and is oriented N. 70° E. Core rocks are separated from structurally higher rocks by the low-angle, outward-dipping Catalina detachment fault (Dickinson, 1991), which is typically marked by a mylonite zone as much as several meters thick on the southwest flank of the domes.

22.5 Junction of I-10 and Az. Rt. 83. Take Rt. 83 south toward Sonoita. Mount Fagan (north end of the Santa Rita Mountains) is on the west and the Empire Mountains are on the east (figs. 1 and 2). Tower on the skyline of the Empire Mountains is NOAA doppler radar.

Empire Mountains

The highest and most rugged part of the Empire Mountains consists of generally southeastward dipping Paleozoic carbonate rocks and quartzite that have been intruded by early and late Laramide-age granitoid plutons (fig. 1). Precambrian granitoid rocks are exposed on the north flank of the Empire Mountains. Sedimentary rocks of the Lower Cretaceous Bisbee Group surround the Empire Mountains and overlap both the Paleozoic and Precambrian rocks (Schafroth, 1965; Finnell, 1974; Drewes, 1980).

The mineralization of the Empire mining district is probably genetically associated with intrusion of the Laramide-age granitoid rocks into the Paleozoic carbonate rocks. The mineral deposits are chiefly oxidized silver-lead and copper minerals contained in vein and replacement deposits. Some mines in the district produced small amounts of gold (Tenney, 1929).

Deposits of argentiferous lead and copper ores were first discovered in the Empire mining district in the late 1870's (Schrader, 1915; Tenney, 1929), but mining became economically feasible only after railroads were built in the region in the early 1880's. The principal camps in the district were California camp, Total Wreck, and Copper camp.

For a time, Total Wreck was the leading silver bullion producer in the Territory. The name Total Wreck came from the description of the site on the first silver mining claims in the Empire Mountains, given by John T. Dillon who discovered the deposits in 1879. He said the site was "a big ledge, but a total wreck, the whole hillside being covered with big boulders of quartz which have broken off the ledge and rolled down" (Granger, 1960). By 1883 the camp had 200 inhabitants and the Tucson Weekly Star reported that there were five saloons, three general stores, a butcher shop, a shoemaker shop, and from eight to ten Chinese laundries. The mine was closed in 1884 after producing about \$500,000 in silver bullion. In 1926 the mill-tailing pile was leased and more than 1,000 tons of low-grade material were shipped as flux (Tenney, 1929).

34.0 Road to Rosemont Junction on the west

Rosemont

Rosemont camp, 4 km to the southwest where copper and minor silver and zinc were mined, was the site of the Rosemont Mining and Smelting Company in the 1880's and 1890's (fig. 2). It was a thriving village in the Helvetia mining district, with about 150 residents, a school, a hotel, and some stores (Sherman and Sherman, 1969). The claims and smelter were acquired by Lewisohn Brothers of New York City in 1896. Subsequently, the mines were worked on an exploratory basis until 1907, when they were closed and the smelter was shut down. After that, Rosemont was more or less deserted (Schrader, 1915).

The American Smelting and Refining Company (ASARCO) acquired the patented mining claims and undertook an exploratory drilling program that demonstrated the presence of a porphyry copper deposit at relatively shallow depth. They planned to develop an open pit mine and to begin mining in about 2020 when

their mine on the eastern edge of the Sierrita Mountains in the Santa Cruz Valley to the west is projected to play out. However, to develop the property adequately they need to negotiate a land trade with the U.S. Forest Service (USFS) to acquire land as far north as Mount Fagan (fig. 2). The future of the project is uncertain because of the drop in the price of copper in late 1998, and because of opposition from residents in the Sonoita area and from environmental groups.

34.7 Base of Sonoita Valley basin-fill alluvial sediments overlying red conglomerate. From a few miles south of I-10 to this point, we have traversed a complexly faulted terrane composed in part of the upper plate rocks of the Catalina detachment fault (fig. 1). Now, as we drive up out of Davidson Canyon we come to the base of the basin-fill sediments of this part of the Sonoita Valley, overlying Upper Cretaceous conglomerate in angular unconformity. An obscure northeast-trending fault separates the higher Sonoita Valley from the lower Davidson Canyon.

36.6 Note dip of bedding to the south in Pliocene basin-fill alluvium in road cuts. The age of the alluvium is estimated to be Pliocene based on the combination of degree of induration, color, and minor deformation.

37.9 View of Sonoita Valley. The Whetstone Mountains lie to the east; the Mustang and Huachuca Mountains to the south; Mt. Wrightson in the Santa Rita Mountains is to the west (fig. 2).

Whetstone Mountains

The Whetstone Mountains, as summarized by Drewes (1996), consist of a sequence of Paleozoic and Lower Cretaceous sedimentary rocks overlying a largely granitoid Proterozoic basement in a little-deformed and sparsely intruded, westward-dipping structural block. Two small granite stocks and a thick granite sill (all 76 Ma) intrude the Paleozoic and Cretaceous rocks. Rhyolitic intrusive rocks form many sills in the Bisbee Group; several are as much as 460 m thick. Mineral resources are base-metal skarn and polymetallic vein deposits, a copper-molybdenum porphyry, a fluorite vein, quartz deposits for flux, and occurrences of uranium, tungsten, and gypsum.

39.0 Greaterville Road on the west.

Greaterville gold placer mining district

Placer gold was discovered on the east side of the Santa Ritas in 1874 and a moderate-sized gold rush ensued (Schrader, 1915; Tenney, 1929). By 1878 there were about 500 people, both Mexicans and Anglos, in the new community of Greaterville (fig. 2). There were several dance halls, saloons, and stores; and the jail was a round hole dug in the ground into which prisoners were lowered by rope (Sherman and Sherman, 1969). However, the Greaterville placer district suffered from a problem common to many southwestern placer deposits - lack of water. Placers were worked by rocker and long tom (low-water-use mechanical devices for separating materials of differing densities). Water was brought 6 km from Gardner Canyon on the south in canvas and

goatskin bags on burros, with the Mexicans charging about 3 cents a gallon for it (Sherman and Sherman, 1969).

Between 1881 and 1886, the camp gradually declined as the richer gravels were worked out and attacks by Indians continued to be a threat. There was a revival of interest in the Greaterville placers between 1900 and 1905 when there were several attempts to bring water in by ditch and pipeline. The center for one of these operations was Kentucky Camp in Kentucky Gulch. From 1905 to about 1930, various companies attempted to work the gravels with a steam shovel, drag-lines, and a dredge; all failed because of insufficient water and poor sampling (Tenney, 1929). Recreational gold panning is a common weekend activity. A discussion of the geology of the Greaterville gold placer district was given by Cox (1992)

42.7 Gardner Canyon Road on the west (access to Kentucky Camp).

Kentucky Camp

Kentucky Camp, about 8 km to the west, was built in 1904 in conjunction with an engineering project to bring water from the Santa Rita Mountains to the gold placer workings in Kentucky Gulch. Five of the original adobe buildings have survived because they were kept in repair until the 1960's by a rancher who bought the property for taxes. The buildings presently are being stabilized by the U.S. Forest Service for possible restoration some time in the future.

46.5 Junction of Az. Rt. 83 and Az. Rt. 82 in Sonoita (fig. 2). Make a 0.8-km loop west on Rt. 82 to the rest area on the south side of the road and return.

47.0 Sonoita; go east on Az. Rt. 82.

Sonoita

Sonoita was established in 1882 on the newly built railroad line. The name comes from the Tohono O'Odham word meaning "place where corn will grow" (Granger, 1960).

54.2 Panoramic view north to the Rincon Mountains. Rain Valley lies ahead to the east with the Whetstone Mountains on the north side of the valley and the Mustang Mountains on the south (fig. 2).

60.5 The cliffy exposures in the Mustang Mountains to the south are composed of three stacked Jurassic welded tuff units which were interpreted to be outflow tuff sheets of the Montezuma caldera (southern Huachuca Mountains), the Turkey Canyon caldera (northern Huachuca Mountains and southern Canelo Hills), and the Parker Canyon caldera (southern Canelo Hills) (Lipman and Hagstrum, 1992).

63.5 San Pedro Valley overview and Stop 1.

STOP 1 -- UPPER SAN PEDRO VALLEY: surficial deposits, gravity, and EM

Regional setting

From this point on the western edge of the upper San Pedro Valley we can see the Whetstone Mountains directly to the north and the Mustang Mountains on the south. The Huachuca Mountains are the next range south across the Babocomari River (fig. 2).

The following description of the Huachuca Mountains is from Drewes (1996). The Huachuca Mountains are underlain mostly by Paleozoic and Mesozoic rocks that overlie a Proterozoic granitoid basement and are intruded by large Jurassic and small Late Cretaceous granitic bodies (fig. 1). These rocks are cut by thrust faults, by northwest-striking steep faults that are splays of the Sawmill Canyon-Kino Springs fault system, and by many other minor faults. Mineral resources of the Huachucas include base and precious metals in polymetallic replacement deposits along minor northeast-to east-striking faults, tungsten minerals in northwest-striking quartz veins, and placer gold.

Sierra San Jose is the high mountain to the south-southeast in Sonora, Mexico. Its elevation is about 2,350 m.

The Mule Mountains are across the valley to the southeast. The famous Bisbee porphyry copper deposits and the Warren mining district are located at the southern end of the Mule Mountains (fig. 2).

The Tombstone Hills, a major silver mining district in the late 1880's, are directly to the east in the middle of the valley (figs. 1 and 2). The Tombstone Hills volcanic rocks have been reinterpreted to be the eroded remnant of a Late Cretaceous caldera (Moore, 1993). The caldera rocks are flanked on the south and east by Paleozoic sedimentary rocks, by Mesozoic Bisbee Group sedimentary rocks, and by Tertiary volcanic intermediate rocks.

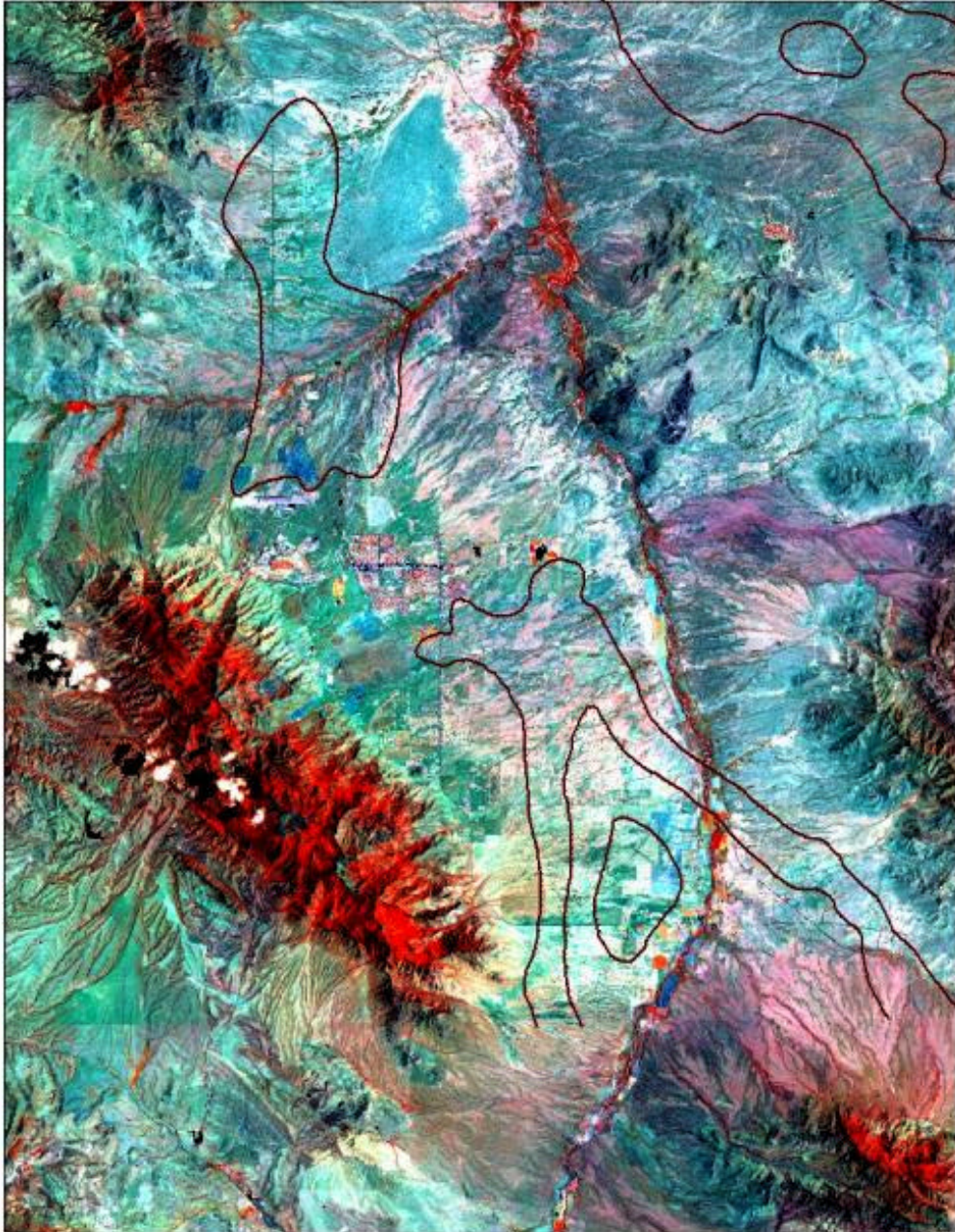
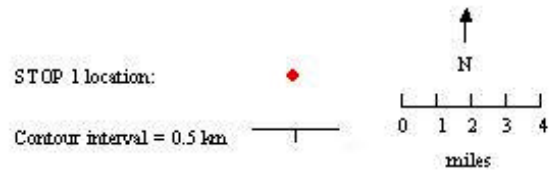
The Dragoon Mountains to the northeast were the site of an Apache stronghold named for the Apache chief, Cochise. A large Miocene stock in the mountains is called the Stronghold Granite (figs. 1 and 2).

Surficial geology and geomorphology

One of the least obvious elements of the upper San Pedro Valley from this vantage point, indeed from anyplace on the western side of the valley, is the San Pedro River itself. Neither the river nor the cottonwood/willow riparian gallery forest that it supports is visible. Our investigation of the locations and shapes of the structural subbasins of the upper San Pedro basin (Gettings and Houser, 1999) helps to explain this topographic anomaly. Using gravity and magnetic anomaly data (described below), well data, and geologic mapping, we defined three structural subbasins of the upper San Pedro basin between St. David and the international border. Figure 3 shows the approximate locations of these subbasins drawn on a thematic mapper (TM) image.

The southwestern part of a large subbasin is shown east of the river and north of the Tombstone Hills and the other two subbasins are shown on the west side of the San Pedro River. Those west of the river are the Huachuca City subbasin north of Sierra Vista and the Palominas subbasin south of Sierra Vista.

**Figure 3. Thematic Mapper
image of the Upper San Pedro Valley**



Gradual subsidence (probably tectonic) of the subbasins west of the river during the Quaternary has warped the eastward sloping piedmont surface on the western side of the valley between the river and the Whetstone and Huachuca Mountains. The slope of the western half of the piedmont surface adjacent to the mountains has been steepened somewhat, but more importantly, the slope of the eastern half of the surface, between the center of the subbasin and the river, has been reduced. Thus, the normal network of streams on the eastern half of the piedmont slope has gradually been disrupted and reduced in number. This has resulted in the development of calcium carbonate-capped mesas on the back-warped piedmont slope adjacent to the river. It is the location of these mesas that obscures the view of the river from the west. On figure 3, the mesa associated with the Huachuca city subbasin is the triangular blue area about 6.5 km (4 mi) wide just east of the constriction near the middle of the subbasin. The mesas associated with the Palominas subbasin comprise a linear feature that extends from about 2 km (1.5 mi) north of the northern end of the subbasin, down along the river to the point on the south where the San Pedro River crosses the subbasin boundary.

The white areas on the TM image between the river and the mesas represent Quaternary calcareous sediments and calcite and gypsum deposits of springs, seeps, and marshes (Haynes, 1987) that form where ground water leaks out along the face of the mesa. This ground-water leakage may have serious consequences for the proposed location of Sierra Vista's ground-water recharge facility. The waste water treatment plant is the black area surrounded by red dots in the center of figure 3. The planned recharge facility was sited between the waste water treatment plant and the escarpment at the edge of the mesa on the assumption that the water would move down through the basin fill to the ground-water table, and then move northeastward perpendicular to the presumed slope of the potentiometric surface to recharge the San Pedro. However, our work suggests that because of the warping of the basin fill and of the overlying surficial materials, the surface of the ground-water table is virtually horizontal between the recharge area and the edge of the escarpment. The recharged water will most likely emerge along the face of the escarpment and evaporate without reaching the river. Additionally, the airborne electromagnetic data discussed below in the section on geophysical studies suggests that near the river the basin fill is clay rich and may be too impermeable to permit the recharge water to reach the ground-water table.

Upper San Pedro Valley geophysical studies

The issues are: (1) discovered and undiscovered mineral resource occurrences and their effect on both ground-water quality and future development; and (2) geologic and structural controls in the basin that affect ground-water quantity. During the course of these studies, surficial and borehole geologic studies and geophysical methods have been used to define the shape of the basins, the character of fill, the probable lithology of underlying bedrock, and the location of geologic structures which offset or otherwise influence the basin fill.

Gravity-anomaly modeling

Gravity-anomaly modeling, constrained by geologic mapping and well data, has been used to define the subbasins and depth to bedrock. Considerable effort has been expended to distinguish unconsolidated basin fill from consolidated conglomerate, as the latter is a poor aquifer. A combination of aeromagnetic- and gravity-anomaly analysis is used to estimate depth to pre-basin-fill bedrock. Then gravity-anomaly analysis constrained by well data is used to map the contact between the consolidated and unconsolidated basin fill.

Physiographically, the upper San Pedro basin is a large basin with exposed bedrock in its middle (Tombstone Hills) (fig. 1 and 2), but the analysis of our study shows that, geologically, it is a series of subbasins separated by saddle-like bedrock highs (fig. 3). A curious feature, common in many basins of the southern Basin and Range Province, is that the river (topographic valley center) doesn't follow the gravity minima that define the deepest parts of the basin.

A bedrock high between the Huachuca City subbasin and the Palominas subbasin underlies the area of major urban development in the vicinity of Fort Huachuca and Sierra Vista (fig. 3). This includes the well fields, sewage treatment plants, and recharge facilities (Gettings and Houser, 1999). Depth to bedrock in this area is less than 250 m and rarely exceeds 500 m, based on well data. Thus, ground subsidence within the urban area from pumping may be a problem, in addition to there being a relatively small aquifer volume.

A major subbasin is present between Tombstone and the Dragoon Mountains (northeast part of figure 2). Analysis of the magnetic- and gravity-anomaly data requires that a substantial part of the subbasin fill is older sedimentary rocks interbedded with mid-Tertiary volcanic rocks (Gettings and Gettings, 1996).

The Tombstone caldera subcrop is well defined by the gravity and magnetic anomaly data. Within the caldera there is a good, deep conductor that may be the intracaldera tuff (see discussion below of the electro magnetic survey). The hydrologic implications of this remain to be determined, but the ring fault may be a barrier to subsurface flow.

The relationship between Laramide-age intrusive rocks and porphyry copper deposits in the Whetstone Mountains, Tombstone Hills (figs. 1 and 2), and elsewhere suggest that the shallowly buried intrusions on the west side of the Tombstone caldera could host another deposit similar to Tombstone. Moreover, the south end of the Huachuca range is a good prospect for mineralization associated with the Montezuma caldera (Lipman and Hagstrum, 1992; Hon, K., 1998, written communication). Should a large mineral deposit be discovered here or immediately across the border in Sonora, there could be economic and environmental consequences from development of the deposit that might affect the San Pedro River.

As of 1999, we are beginning a similar study on the lower San Pedro basin from Benson northward to the junction of the San Pedro River with the Gila River. Project completion is scheduled for Oct. 2001.

Airborne ElectroMagnetic survey of Fort Huachuca vicinity, upper San Pedro basin

An airborne time domain electromagnetic survey (AEM) of the bedrock high beneath Fort Huachuca and Sierra Vista was contracted for by the the Environment and Natural Resources Division of the U.S. Army's Garrison at Fort Huachuca, Arizona and flown in 1997 under USGS direction. Geoterrex-Dighem Ltd. of Ottawa, Canada acquired the AEM data. The survey data were analyzed by the U.S. Geological Survey, Geologic Division. The objectives of the survey were: (1) to define lithologic variations that affect ground-water flow and storage; and (2) to evaluate the use of the time-domain electromagnetic method in the southwest desert setting as a means of mapping depth to water.

The analyses of these data (Bultman and others, 1999) are summarized below. In brief: (1) the location of the shallowest conductor is often closely related to the water table; and (2) the conductivity maps suggest that most of the recharge in the northern part of the survey area is going northward into the Babocomari River rather than eastward across the piedmont to the San Pedro. The deeper conductors or thicker conductors indicate areas of fine-grained facies containing volumetrically significant clay and silt fractions. These act as aquatards and affect hydraulic behavior, as well as reducing available reservoir volume. Much of the eastern half of the survey area falls in this category.

Figure 4 shows the flight lines that comprise the AEM survey of the upper San Pedro basin. Due to the topography of the region, the direction of the flight lines for the southwest part of the survey is perpendicular to the majority of the survey, creating two sets of parallel flight lines. The northeast trending lines are the flight lines used in this analysis. Figure 4 also displays the unconsolidated sediments of the basin, consolidated conglomerate that may be equivalent to Tertiary Pantano Formation in nearby basins (called Pantano? here, after Gettings and Houser, 1999), and bedrock.

The sediment fill of the upper San Pedro basin based on CDT data

Conductivity-depth transform (CDT) data provide information on the conductivity of sediments within the basin. By combining all the vertical CDT profiles into a data cube, it is possible to visualize the conductivity of sediment fill in the basin. If it is assumed that clays and silts in the upper San Pedro basin are more conductive than sands and gravels, it then becomes possible to map these units within the basin. If these clays and silts are less permeable and porous than sands and gravels, we can also make hydrological interpretations based on the CDT data.

The CDT data shown in figures 5 through 7 include cross sections of, and a near horizontal slice through, the data cube. For each cross section, the top of the data indicates the ground surface. Black areas below the data indicate areas where the signal was lost. Areas where the signal was lost also appear as black holes in the near-horizontal data slice in figure 7. Loss of signal generally occurred under shallow conductive rock or under cultural anomalies. Conductive rocks dissipate available energy and cultural features produce large amounts of electromagnetic noise. Bedrock is encountered only on the southwestern, northeastern, and eastern margin of the data. In the central portion of the basin, and at the northern and southern margins of the data

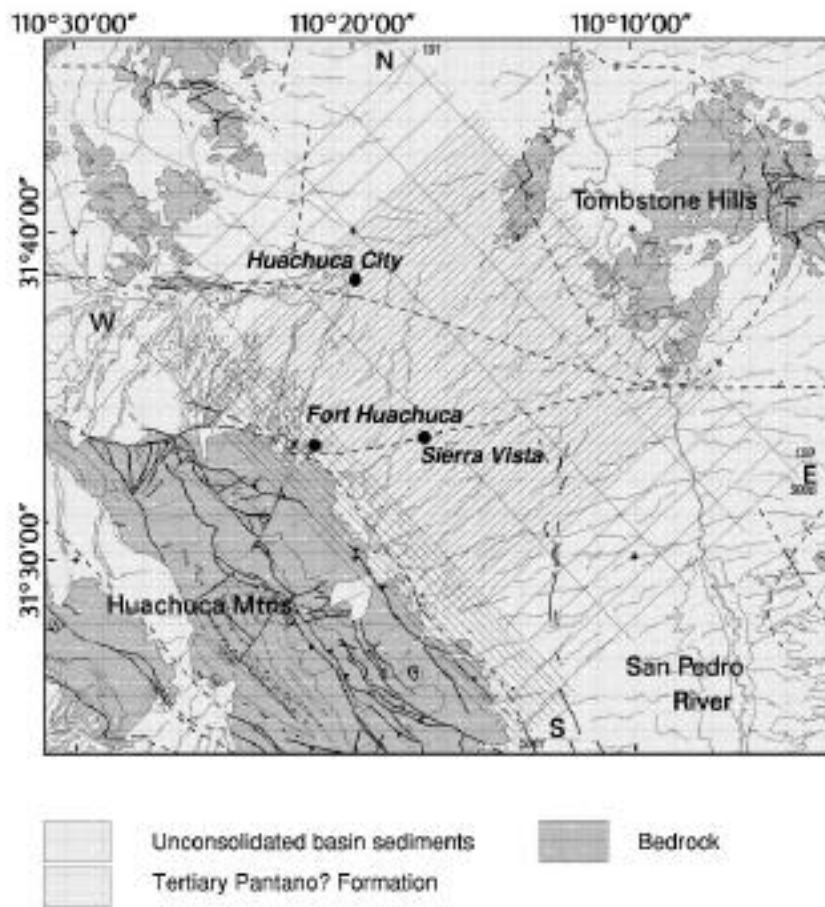


Figure 4. Locations of airborne electromagnetic flight lines in the upper San Pedro Valley near Ft. Huachuca and Sierra Vista

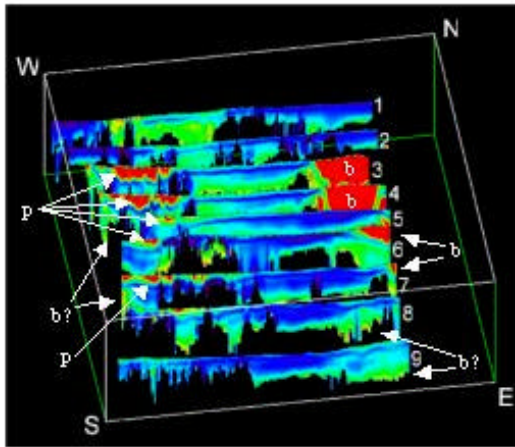


Figure 5. View of conductivity-depth transform cross-sections parallel to flight lines

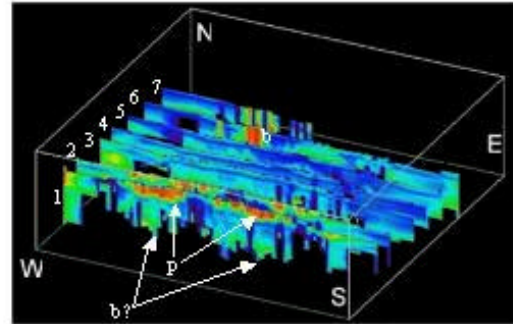


Figure 6. View of conductivity-depth transform cross-sections perpendicular to flight lines

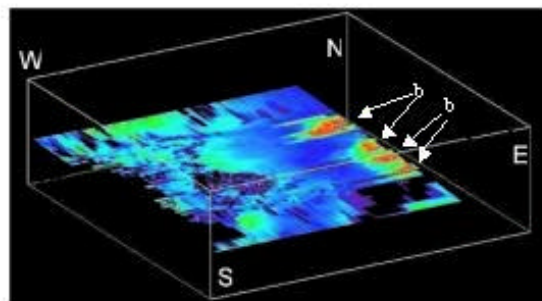


Figure 7. View of slice through conductivity-depth transform data cube taken approx. 100m below ground surface

Explanation for figures 5 through 7:

Areas labeled with “b” indicate exposed bedrock

Areas labeled with “b?” indicate possible concealed bedrock

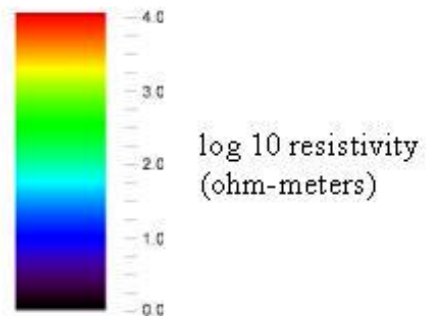
Areas labeled with “p” indicate Pantano? Formation rocks

Dimensions of data cube outline (shown surrounding CDT data):

Z: 1.5 km

W to N: 28.5 km

W to S: 32.0 km



cube, bedrock lies deeper than the approximately maximum 400-m depth of resolution of the AEM data.

Figure 5 is a visualization looking at cross sections of the data cube viewed from above and to the north-north west. The cross sections are numbered and are parallel to the flight lines. All cross-sections display an upper resistivity minimum as a blue band near the surface. This feature is discussed later. In cross sections 3 through 7, highly resistive rocks of the Pantano? Formation (labeled “p”) can be seen at the surface to the west and the highly resistive bedrock of the Tombstone Hills can be seen to the east (labeled “b”). The bedrock associated with the Huachuca Mountains is at depth to the west. Cross sections 8 and 9 indicate that the (b?) bedrock associated with the Tombstone Hills may extend to the southeast, concealed by basin sediment. Thick regions of low-resistivity rock are evident to the north, west, and south of the Tombstone Hills. In the northern part of the basin, these rocks thin to the west and thicken to the south. They probably represent silt and clay deposited from the weathering of volcanic rocks of the Tombstone hills. The lower part of this wedge may include outflow tuff from the Laramide-age Tombstone caldera.

Figure 6 is a visualization looking at cross-sections of the data cube viewed to the north. In this figure, the cross-sections are taken perpendicular to the flight lines. The block has been rotated slightly counter-clockwise from the previous visualization. Cross-sections 1 and 2 display the resistive rocks of the Pantano? Formation at the surface. These are labeled with “p” on figure 6. Possible bedrock is labeled with “b?” in this figure. The upper resistivity minimum (or conductive layer) can be seen near the surface of cross-sections 3, 4, 5, 6, and 7. This feature becomes much thicker to the east and southeast, indicating that the silt and clay content of the sediments increases at depth in these directions. Finally, in cross sections 6 and 7, the very resistive bedrock associated with the Tombstone Hills is evident. The Sierra Vista bedrock high can be seen as a near-surface area of high conductivity near the center of cross section 2.

Figure 7 is a slice through the data cube that is viewed from above looking in a northerly direction. This slice dips slightly to the northeast to parallel the slope of the ground surface. The depth of the slice is about 100 m below the ground surface. Areas that appear black on the slice are regions of no data for the elevation of the slice. The highly resistive bedrock of the Tombstone Hills (b) can be seen to the northeast. At this depth, the sediments that are near, but not abutting, the Tombstone Hill bedrock are very conductive, probably silt and clay deposited from the weathering of the volcanic rocks of the Tombstone hills in what might be interpreted as a low energy environment. These grade to more resistive sand and gravel sedimentary facies in the west in what may be interpreted as a higher energy environment. Based on observations made from the CDT data cube, much of the southern and eastern areas of this AEM survey likely contain silt and clay at depth and may represent a poor aquifer with limited permeability and porosity.

The upper resistivity minimum

To test the hypothesis that the upper resistivity minimum may be related to the water table, we used nine test wells where we had resistivity logs (16 foot lateral logs) and water-table information. This allowed us to plot the water table, the CDT vertical

profiles, and the well resistivity log together for comparison. These nine plots are shown in figure 8 a-i.

These plots demonstrate some interesting relationships between the digital CDTs, the well resistivity logs, and the water table. (1) The digital CDTs consistently demonstrate a higher resistivity throughout the profile than the well log. (2) The shapes of the CDTs match the general shapes of the well logs in many case for the first 150 meters depth. That is, if the well logs were to be smoothed with a smoothing filter, their shapes would be similar to the CDTs in many cases. (3) For many of the test wells, the water table lies within a small distance from the upper resistivity minimum of the CDT data. This is not true in test wells 1 and 2 which were drilled in the highly resistive consolidated conglomeratic Tertiary Pantano? Formation. All other test wells were drilled in unconsolidated basin sediments. The digital CDTs at test wells 1 and 2 display extremely high resistivities at the ground level and display an upper resistivity minimum slightly below the water table in test well 1 and about 80 meters below the water table in test well 2. In areas of highly resistive rock at the surface, the upper resistivity minimum does not seem to be correlated to the water table. Test well 6 also displays the upper resistivity minimum below the water table, about 40 meters in this case. All of the other test wells have a digital CDT upper resistivity minimum within one vertical data increment (11.7 meters) of the water table. In general, in the geographic region of the test wells where Pantano? Formation is not present (to the east of Fort Huachuca into the central portion of the AEM survey) the digital CDT upper resistivity minimum seems to be fairly well correlated with the water table. It is possible that this is due to more conductive, less permeable sediments controlling the location of the water table. (4) The digital CDT resistivity profiles seem well correlated with actual resistivity to depths of about 150 meters. At depths greater than this, conductive features seem to be conservatively estimated or underestimated.

The upper resistivity minimum map

The upper resistivity minimum can be found for all digital CDT data points in the survey, gridded and mapped. As shown above, this feature may provide a good representation of the location of the water table in some cases. The upper resistivity minimum map for the 1997 upper San Pedro AEM survey is shown in figure 9. A number of adjacent high and low values are due to cultural noise in the Sierra Vista area and are labeled in figure 9. Many of the other speckled looking features leading from western Sierra Vista to the northwest are also probably due to cultural interference in the AEM data. Gravity and magnetic survey data (Gettings and Houser, 1999) indicate that there is a bedrock high almost directly under the city of Sierra Vista. If the AEM data are seeing through the cultural noise at all, it indicates that this may act as a perch for the water table in this area. The very resistive Pantano? Formation is clearly visible and is indicated by several arrows pointing to outcrops of this formation. North and east of the Sierra Vista bedrock high is a region where possible clay and silt sediments form the upper resistivity minimum and possibly keep the water table high. It is in this region that the upper resistivity minimum was highly correlated with the water table in the test wells. To the west of this region, and to the east of the indicated Pantano? Formation, is an area of lower elevation for the upper resistivity minimum. This region

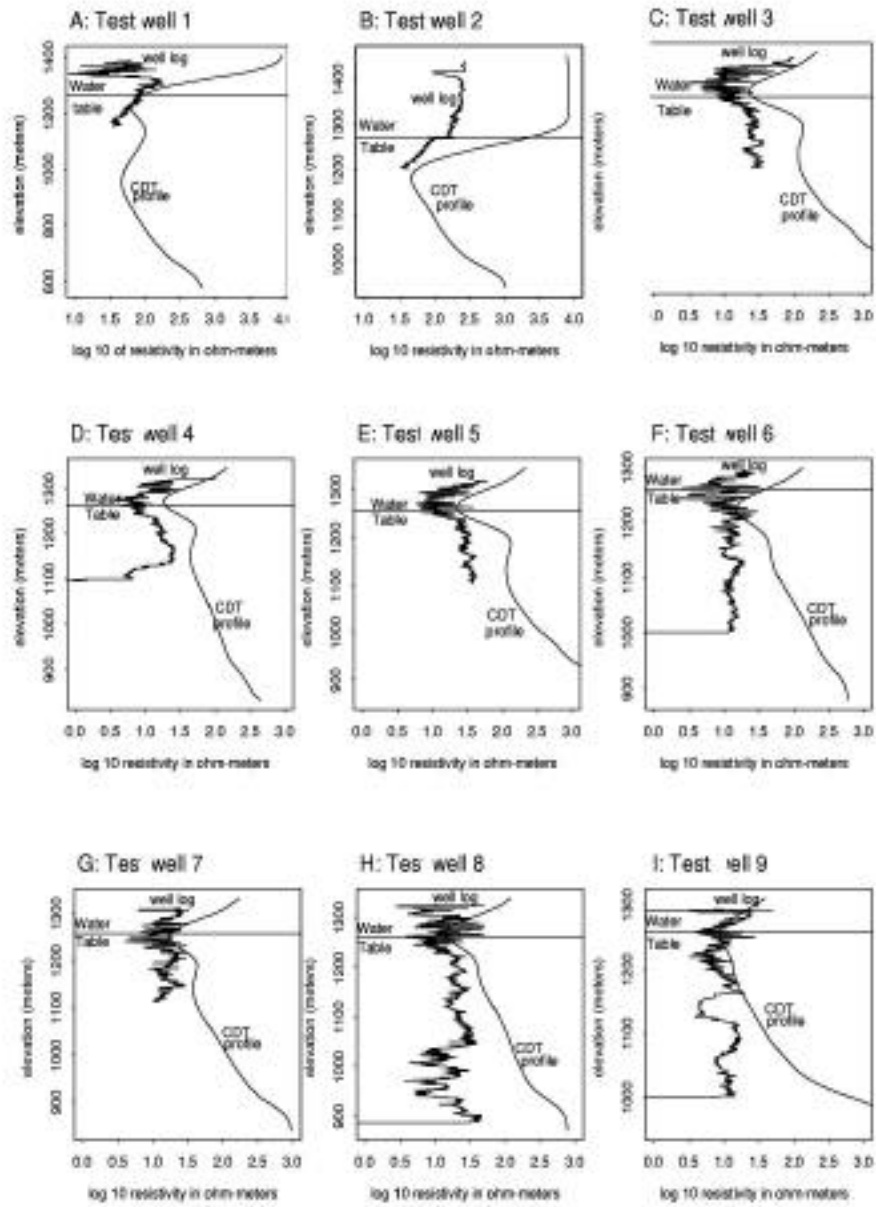


Figure 8. Resistivity measured in nine test wells compared to conductivity-depth transform profiles (where conductivity has been converted to resistivity).

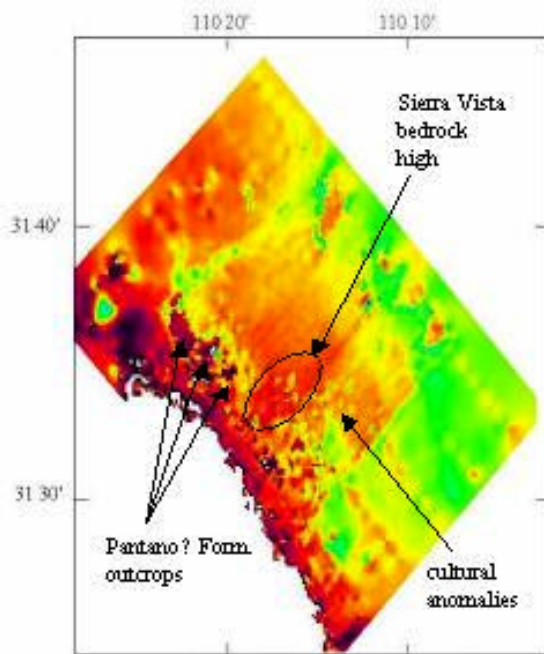


Figure 9. Map showing relative Elevation of upper resistivity
Minima

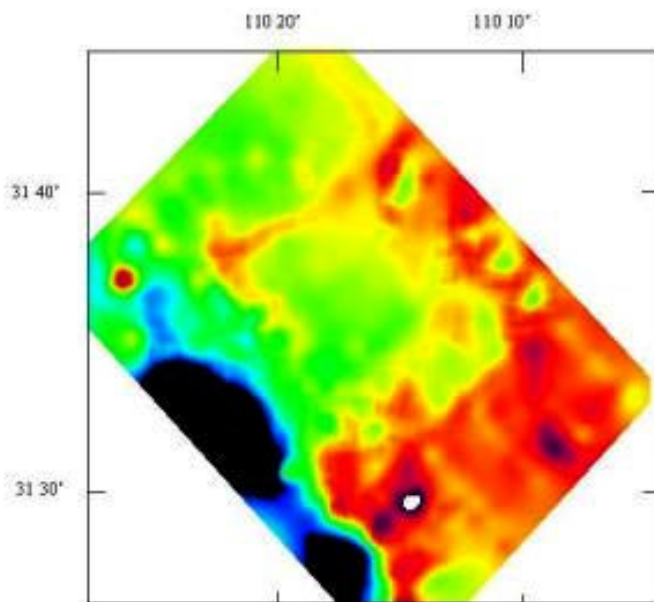
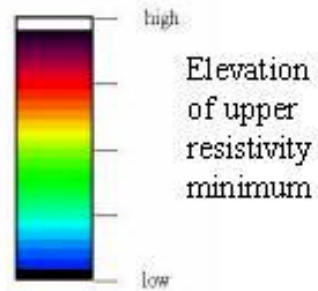
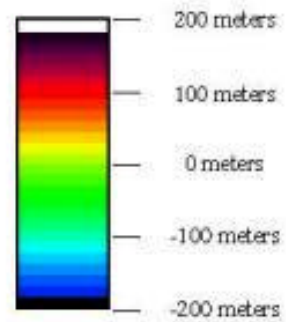


Figure 10. Water table elevation minus the smoothed upper resistivity minimum Map.



may be related to the thinning and disappearance of clays and silts and(or) to a lowering of the water table.

In order to compare the upper resistivity minimum map with the water table, we smoothed the upper resistivity minimum map with a half-kilometer radius smoothing algorithm to generalize it and to help minimize cultural anomalies. The 1998 well-water-level data (Tatlow, 1998) were then gridded with a minimum curvature routine to produce a grid of the water table elevations. The smoothed upper resistivity minimum map was then subtracted from the water-table grid resulting in figure 10. This figure shows that the upper resistivity minimum map does a good job of approximating the water table in the central portion of the basin. In the west, where resistive high energy facies rocks are present, it tends to overestimate the elevation of the water table. In the east, it tends to underestimate it. For unknown reasons, the water table is drastically underestimated in the south-central portion of the map, where the water table minus the upper minimum resistivity map approaches 200 m.

63.5 Turn around and head back west on Az. Rt. 82.

71.5 Turn south onto the Elgin Road.

76.1 Village of Elgin (fig. 2). Cross the bridge and turn left.

76.8 Bear right.

78.8 The Sonoita Winery and vinyards. The red soil and climate of this area are said to be similar to those in wine producing regions of France.

80.7 Junction with Az. Rt. 83. Turn left.

84.9 Huachuca Mts. to the southeast.

86.3 Az. Rt. 83 turns to the west to Canelo (fig. 2). Continue straight ahead to the south toward Canelo Hills.

Canelo Hills

The Canelo Hills (figs. 1 and 2) are composed chiefly of two Jurassic rhyolite tuff units, as much as 300 and 2,000 m thick, that are partly welded, to densely welded, to fluidal (Hayes and Raup, 1968; Simons, 1974; Lipman and Hagstrum, 1992). The tuffs enclose large blocks of Paleozoic sedimentary rocks that have been interpreted by Lipman and Hagstrum (1992) to be intracaldera megabreccia lenses. Geologic features favorable for ore deposition are uncommon in the Canelo Hills (Drewes, 1996).

The Canelo Hills were first shown on an 1896 map as the Canille Mountains (Granger, 1960), and the school at Canelo (now abandoned) is shown as Canille School on the O'Donnell Canyon 7.5-minute quadrangle. The accepted name on the range is now Canelo, which means cinnamon tree in Spanish and perhaps was descriptive of the color of the hills (Granger, 1960). On the other hand, one of the meanings of canille in

Spanish is rib (as in a fabric), which may have been descriptive of the topography inasmuch as the Canelo Hills consist of a series of long, narrow faulted ridges.

89.1 Arizona Hiking Trail crosses the road. From here to about the next 0.3 mi the road crosses a megabreccia block of Paleozoic limestone and quartzite that both overlies and is surrounded by welded tuff.

89.9 Canelo Pass, elevation 1,599 m. Between Canelo Pass and the San Rafael Valley, the exposures along the road are of densely welded quartz rhyolite tuff (fig. 1). These rocks are part of the intracaldera fill of the Parker Canyon caldera of Lipman and Hagstrum (1992).

90.0 San Rafael Valley overview. This is the valley where the Spanish explorers first entered what is now the southwestern U.S. The inscription on a monument in the valley near the border reads "By this valley of San Rafael Fray Marcos de Niza, Vice-commissary of the Franciscan order and delegate of the Viceroy in Mexico, entered Arizona, the first European west of the Rockies, April 12, 1539." More recently, the valley achieved fame as the site for the filming of the movie *Oklahoma*.

The Patagonia Mountains to the west across the San Rafael Valley (figs. 1 and 2) were described by Drewes (1996) as a granitic terrane, chiefly of Proterozoic, Jurassic, and Late Cretaceous ages. Small areas are underlain by Paleozoic and Mesozoic sedimentary rocks, and Cretaceous or early Tertiary volcanic rocks are common to the northeast. The mineral resources are copper, lead, zinc, molybdenum, manganese, silver, and gold in vein, skarn, polymetallic replacement, and porphyry copper deposits. Some placer deposits have produced minor amounts of gold.

STOP 2 -- SAN RAFAEL VALLEY: The Magnetic-EM-Gamma-Ray (MEG) truck , buried potentially mineralized magnetic anomaly

Introduction

Favorable bedrock that is concealed by shallow sediment fill represents one of the few remaining places that economically viable and strategically significant undiscovered conventional mineral deposits may occur in the contiguous U.S. The truck-mounted magnetometer is a tool that Southwest Field Office personnel have used to assess favorable terrane for these types of deposits. It is ideally suited to finding concealed faults, estimating depth to bedrock, locating anomalies missed by aeromagnetic surveys, and in some cases it can provide information about the lithology of rocks concealed by basin sediments.

The magnetometer is mounted to a truck instead of to an airplane because magnets are dipoles and the resulting geometry causes their associated potential field to decrease proportional to the inverse of distance from the source cubed. Techniques for determining concealed lithology are based on observations of the magnetic texture of a specific lithology, making it is extremely important to acquire all of the magnetic field information possible. This means being as close to the ground as possible.

Currently, only a cesium vapor magnetometer is operational in the MEG truck. The Southwest Field Office is beginning to design and build a digital 60-Hz EM system and digital gamma-ray spectrometer for the truck. The 60-Hz EM instrument may be very useful for ground water applications. The gamma-ray spectrometer will provide a horizontal equivalent to bore-hole logging and will help elucidate basin stratigraphy.

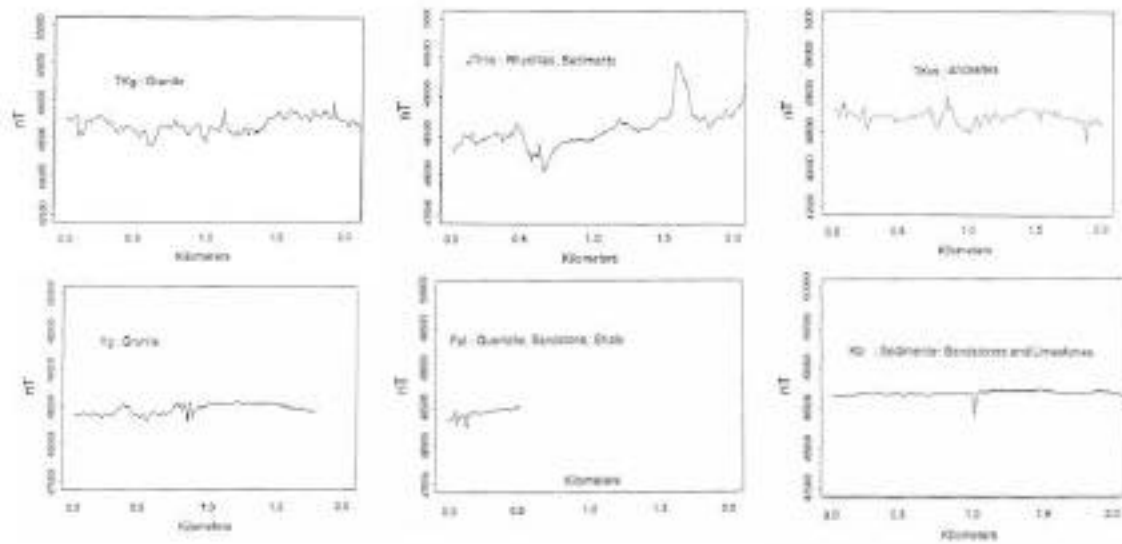
Identifying concealed lithology

Figure 11 shows signals acquired from the truck-mounted magnetometer over several exposed lithologies. Each of these signals has a different texture and the goal is to quantify that texture. The large range of scales over which these magnetic signals manifest themselves means that measures related to fractal scaling are likely to be good estimators of the signal's texture. Figure 11 displays several fractal measures, including fractal dimension, D , that uniquely describe the individual exposed lithologies.

The magnetic texture that is unique to a lithology (its *magnetic signature*) can be used, in some cases, to identify the lithology that is concealed by basin sediment. For this technique to work, the sediment fill must be virtually non-magnetic, the concealed lithology must be very magnetic with a large amplitude signal, and the depth of burial must be less than 100 m. The identification of a concealed lithology begins by first selecting several candidate lithologies based on the magnetic signature of their outcrop and the geological relationships within the region in question. The signal from the candidate lithologies is upward continued to a depth equal to its burial under basin sediment. This simulates the signal's source at the depth of burial. The signal from the basin fill above the concealed lithology is then added to the signal from the upward continued candidate lithology to form a synthetic signal. The synthetic signal is then compared to the actual target signal acquired over basin fill using the quantitative textural measures. It is possible to distinguish very magnetic concealed lithologies from less magnetic concealed lithologies. Also, it is possible to distinguish some of the lithologies with a high amplitude magnetic signature. This can often lower the number of possible choices for the concealed lithology. More research is needed to uniquely identify all concealed lithologies whose magnetic signatures have high amplitude signals.

An example of the application of these techniques to the San Rafael basin

Figure 12 is a TM image showing the San Rafael Valley and the surrounding mountain ranges. These ranges and parts of the San Rafael Valley lie in the Coronado National Forest. Work in the San Rafael basin vicinity was initially done in 1991 and 1992 for the Coronado National Forest Mineral Resource Assessment (CNFMRA). At that time, truck-mounted magnetometer analysis showed that the northern margin of the basin was probably quite shallow and underlain by the mapped andesitic rocks that lie adjacent to basin to the north. The remote sensing study we did for the CNFMRA showed that this volcanic suite is very complex and highly altered, although it contains little known mineralization. Given this setting, and the nearby presence of the Red Mountain (figs. 1 and 2) porphyry copper deposits discussed in a later section, this area was chosen for much of the initial testing of the truck-mounted magnetometer. This work led to the discovery of a large magnetic anomaly that can be modeled as an



Lithology	mean (nT)	variance	std. dev. Magnetic	gamma ratio	D
Tlg	49758.4	17187.0	34.50.3	11.0	1.85
Tls	49637.3	81481.0	3402.0	15.0	1.83
Tls	49710.0	15488.9	25700.3	111.0	1.92
Tg	49820.5	2817.0	939.1	14.7	1.90
Pol	49426.2	3184.2	3021.2	13.0	1.89
Sh	49559.2	20588.6	1395.7	13.5	1.84

Figure 11. Magnetic signatures for individual exposed lithologies.

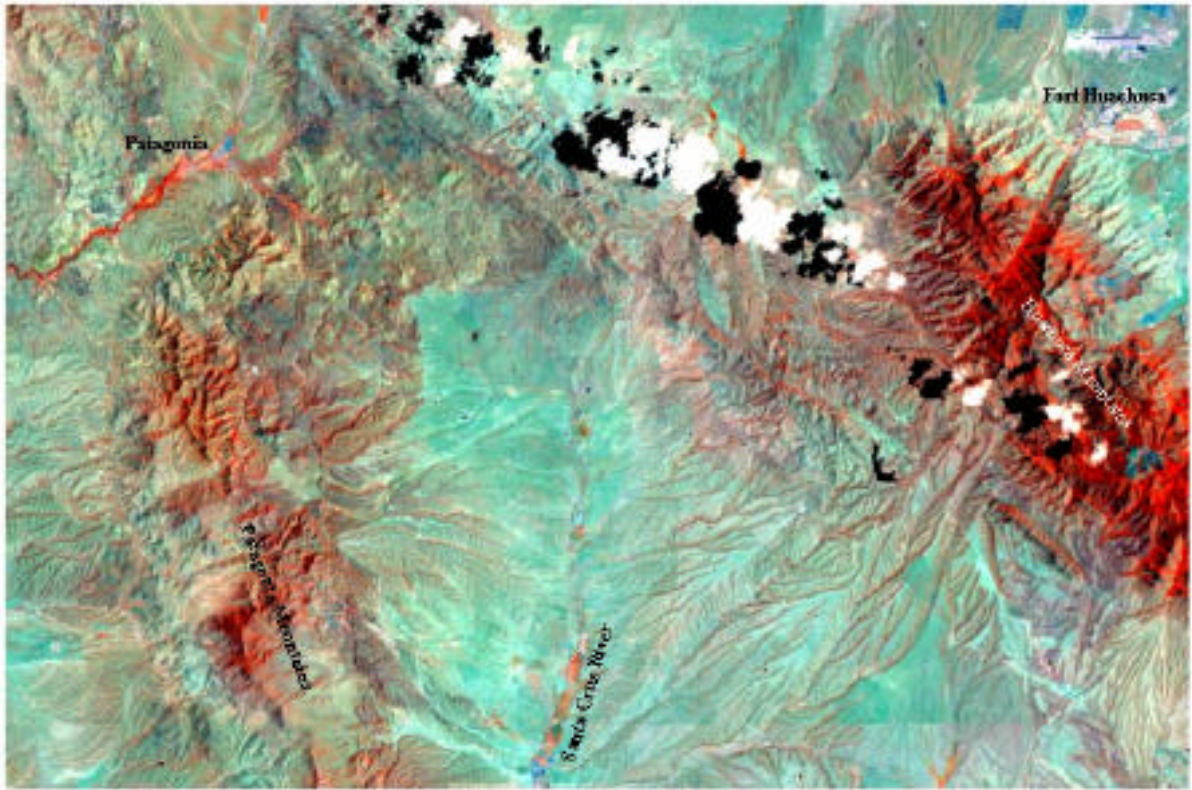
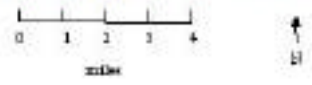


Figure 12. Thematic Mapper image of San Rafael Valley and Patagonia Mountains



intrusion with altered margins. The location of this possible intrusion is shown in figure 13 (labeled TKg) near the northern edge of the basin.

Recently, truck-mounted magnetometer work was integrated with an analysis of gravity and aeromagnetic data in order to summarize the geometry, structure, and concealed lithology of the San Rafael basin. Some results are shown in figures 13 and 14. Estimates of concealed lithology in the San Rafael basin (fig. 13) are ranked according to their degree of certainty. Based on gravity modeling shown in figure 14, the basin has a maximum depth of approximately $1.05 \text{ km} \pm 0.1 \text{ km}$. Figure 13 shows depth contours for the entire basin. At least in its southern part, the San Rafael basin can be modeled as an asymmetric graben faulted on the western margin. The northern part of the basin is structurally more complex and may have high angle faults on its western, northern, and eastern margins.

Based on this analysis, the San Rafael basin has a high potential for concealed mineral deposits on its western and northern margin. In addition, if the upper basin fill has a permeability and porosity similar to the upper basin fill in nearby basins, and if the modeled thickness of upper basin fill is correct, the San Rafael basin contains an aquifer up to 300 meters thick beneath a substantial part of the basin.

91.7 Little Outfit Ranch road on the north.

92.4 Approximate northern margin of anomaly.

93.7 Approximate southern margin of anomaly.

94.3 Santa Cruz River about 10 km south of the headwaters.

94.5 Road junction; go straight.

97.9 Junction with Mowry Road; go straight. Pliocene basin fill in road cut on the right. This is the poorly indurated upper sedimentary unit modeled by M.W. Bultman in the San Rafael basin.

98.3 - 98.8 Exposures of Miocene conglomerate on both sides of the road. This is the indurated lower sedimentary unit modeled by M.W. Bultman in the San Rafael basin.

99.4 Saddle Mountain is on the north; elevation about 1,775 m (figs. 1 and 2). Note stringers of silicic and argillic alteration crossing the terrain.

101.5 Bear right; cross Harshaw Creek.

102.1 The residence of on left side of road is the site of a bedrock well 91 m deep pumping 30 gpm with conductivity of 3.02ms/cm and TDS of 1.50g/l. The well is in altered bedrock.

105.4 join Harshaw Road; bear right

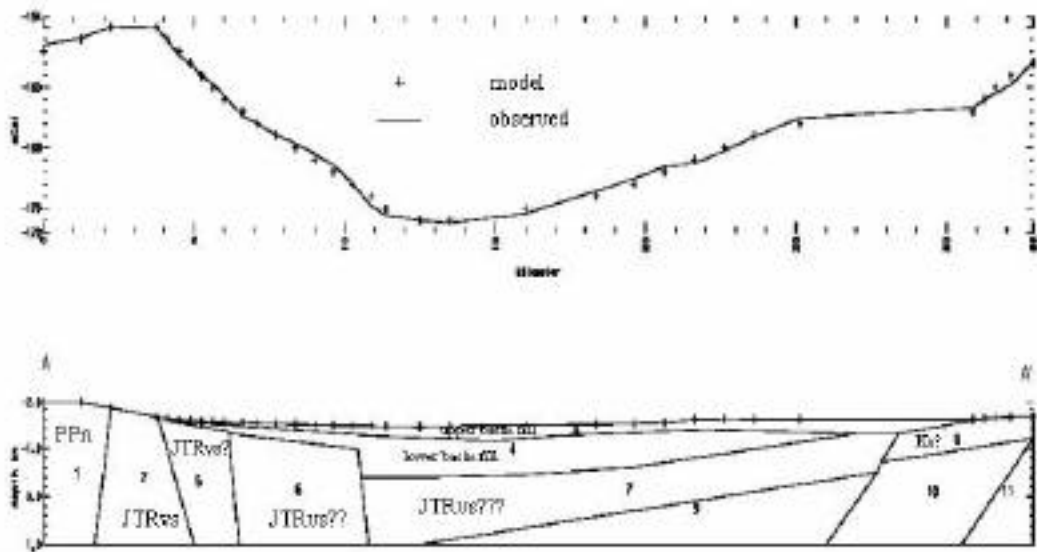


Figure 14. West to east gravity model profile, San Rafael basin

108.8 Patagonia city park at 4th Ave.

STOP 3 -- PATAGONIA CITY PARK: lunch and overviews of region's hydrologic profile and initial results of SW Mineral and Environmental task 3

Patagonia (town)

Patagonia (fig. 2) was established in 1898 when Rollen Rice Richardson bought the land where the town of Crittenden was located and told the residents they had to move about 5 km south to a marshy area that he owned at the present site of Patagonia. Richardson, a rancher, owned much of the land in the area. Richardson had wanted to call the town Rollen, but the residents of the new town chose the name Patagonia from the name of the mountains to the south. Because the petition for a post office had to be signed by the residents (who were not happy about having had to move from Crittenden), Richardson had little say in the matter of the town name (Granger, 1960).

In 1909, Patagonia was an active mining center with about 200 residents. Two daily passenger and mail trains stopped there, and daily stage and mail service was maintained between Patagonia and the mining camps to the south -- Harshaw, Mowry, Washington, and Duquesne (Schrader, 1915). The old train station at the northeast end of the city park is used for city government offices. Nowadays the economic base for Patagonia is diverse and includes ranchers, retirees, hunters, bird watchers, and holistic healers.

Patagonia and Santa Rita Mountains

Location and Physical Setting of Study Area

The study area is located approximately 60 miles southeast of Tucson, in the Mexican Highland Province of southeastern Arizona and lies within the southern Basin and Range Province, which extends from southern Nevada southward into northern Mexico. Within the study area, Sonoita Creek and its tributaries incise the rolling hills between the Santa Rita Mountains and the Patagonia Mountains (fig. 2). The southwestern part of the area drains into the Santa Cruz River near Nogales, Arizona and the southeastern part drains into the headwater streams of the Santa Cruz River in the San Rafael Valley. Waters from Temporal Gulch and Harshaw Creek, two of the larger watersheds in the area, drain into Sonoita Creek from the north and south, respectively. Almost all of the lands underlying the study area are within the Coronado National Forest with the exception of state-owned and private land holdings in and adjacent to the town of Patagonia and a few isolated inholdings surrounding mining claims.

The area is semi-arid, although this part of Arizona is cooler and wetter than the low deserts because of the higher altitude of the region. Hot and dry summers are normally moderated in late July and August by thunderstorms, some of which are severe. The storms commonly produce flash floods. Winter rains are of a frontal nature and generally occur from November to February. Snow melt on the high mountains in

January and February can add to the winter rains and produce streamflow as high as in late summer. Average annual precipitation in the Patagonia Mountains is about 430 mm, approximately 280 mm of which falls in the summer and 150 mm in the winter (fig. 15).

Geologic Setting

The geology of the Patagonia Mountains area was mapped by Simons (1974) and is shown on figure 1. The geology is dominated by a large Laramide-age intrusion of quartz monzonite to granodiorite composition that is approximately 8 km wide at the international border and narrows northward over a distance of roughly 19 km where it is overlain by a volcanic-intrusive complex and north-striking co-magmatic dikes and sills. The oldest wall rocks into which the granodiorite pluton was emplaced include Precambrian biotite-quartz monzonite and hornblende diorite on the east side of the range, along with biotite-hornblende quartz monzonite and hornblende gabbro along the west side. Paleozoic sedimentary rocks are present in two areas on the east side of the range. Mesozoic rocks are present mostly in a north-northwest trending belt through the range and as Jurassic granite intruding the Precambrian rocks on the west flank of the range. These Mesozoic rocks are predominantly igneous and include intermediate to felsic volcanic tuffs and flows and intrusive monzonite, diorite, granodiorite, granite, and syenite. Clastic sedimentary rocks are also present locally. The occurrence of younger Cretaceous and Tertiary sedimentary and volcanic rocks at the northern end of the Patagonia Mountains and the greater width of the intrusion at the south end along the US-Mexico border suggest that the southern part of the area may be more deeply eroded than exposures farther north.

Red Mountain overview -- volcanic stratigraphy and alteration

Quinlan (1986) described the geology and alteration of the Red Mountain porphyry copper deposit. Red Mountain is composed of three Cretaceous through lower Tertiary volcanic sequences that have undergone various degrees of alteration associated with the formation of a porphyry copper deposit. Simons (1974) described the upper sequence as white, light-gray, yellowish-gray, or pale-red, massive, very fine grained to sparsely porphyritic, silicic flow breccia and tuff. This sequence forms most of the upper part of the mountain and is as thick as 730 m. These rocks are locally cliff-forming and outcrops are stained with iron oxide. Alteration of the original volcanic rock to a quartz, kaolinite, sericite, and limonite assemblage is common. Alteration to alunite and zunyite is locally common. Schrader (1915) reported that the tuff is profusely impregnated with pyrite, chalcopyrite, and chalcocite disseminated in crystals and grains. Drewes (1980) gave the age of the rock as Paleocene(?).

The middle volcanic sequence is andesite and trachyandesite about 915 m thick that crops out on the flanks of Red Mountain. This sequence was dated at 72 Ma (Simons, 1974). Hornfels bands occur at the base (Quinlan, 1986). Rocks of the lower sequence are chiefly latitic volcanic conglomerate and breccia, and silicified tuff and flows (?) interlayered with and cut by latite sills and dikes. This sequence is exposed on the south side of Red Mountain in Alum Canyon (fig. 16). It correlates with the Upper Cretaceous silicic volcanics of Simons (1974).

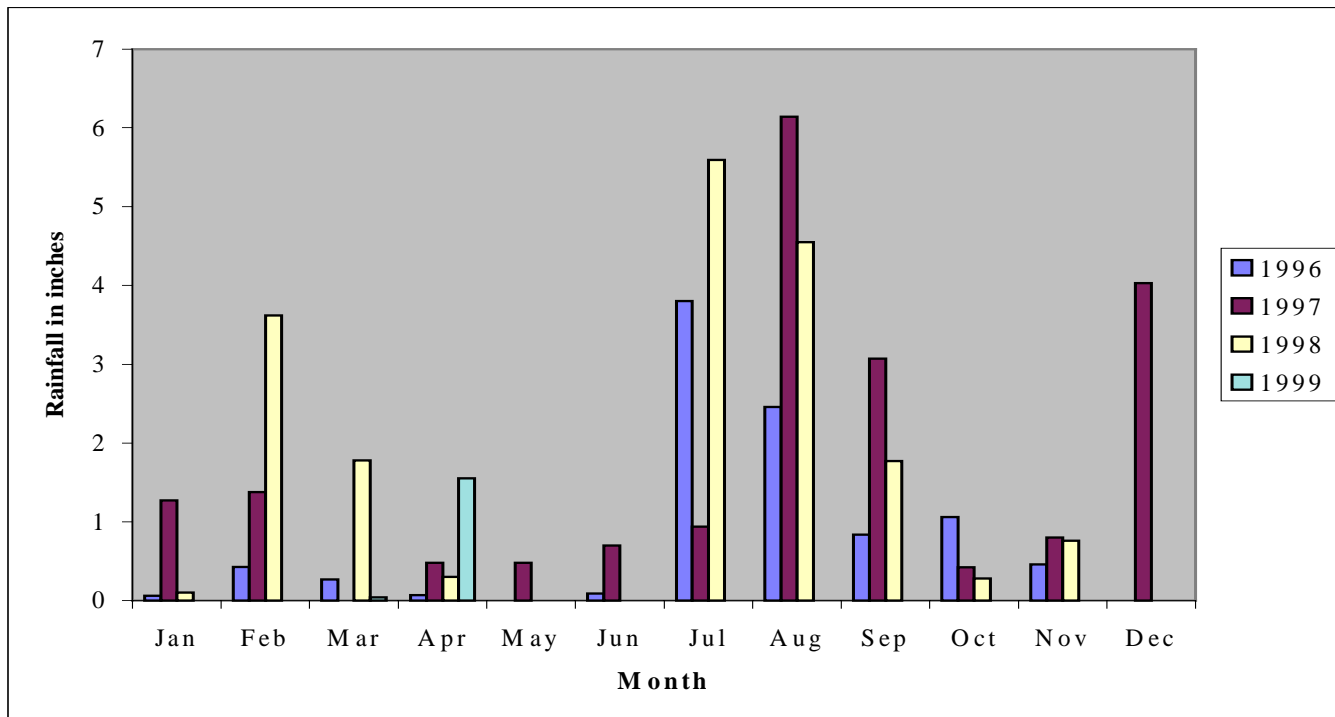


Figure 15. Total monthly precipitation values in the vicinity of the Patagonia Mountains, southern Arizona based on available data.

The rocks of Red Mountain dip to the east at about 15° and are cut by porphyritic granitic dikes and small intrusive bodies of Laramide age.

Mineralization-Mining History

The Patagonia Mountains host at least two porphyry-copper systems and a variety of associated mineral deposits that formed during or immediately after emplacement of the granodiorite system (Corn, 1975; Graybeal, 1984, 1996). Several large pyritic zones centered on Red Mountain and the Sunnyside Mine-Humbolt Canyon area to the south contain pyrite or its oxidized products, primarily in the disseminated form, along with quartz, sericite, alunite, pyrophyllite, and kaolinite along with minor chalcopyrite

Within and adjacent to the area of abundant pyrite are numerous base and precious metal deposits varying in size from scattered prospect pits to mines with important production and metal reserves. The disseminated deposits typically are the largest and include the Red Mountain porphyry copper deposit (Corn, 1975; Quinlan, 1986) and the Hardshell silver deposit (Koutz, 1984). Next in size are the breccia pipe deposits exemplified by the 4-Metals copper deposit (Graybeal, 1973) and the Ventura Mo-Cu deposit. Limestone replacement deposits, including the skarn occurrences at Washington-Duquesne (Lehman, 1978), the large pyritic replacement deposit at the Flux Mine, and the manganese replacement at the Mowry Mine were also significant producers in the area. Sulfide veins with silver minerals are the most numerous and variable in size, of which Trench mine is the most prominent example (Graybeal, 1984).

In the saddle between the Patagonia and Santa Rita Mountains, alluvial sand and gravel deposits locally overlie bedrock (fig. 16). These basin-fill sediments skirt the area, typically in depositional contact with bedrock, but locally, such as at the foot of the Patagonia Mountains south of the town of Patagonia, they are faulted against older rocks (Drewes, 1972a). This predominantly fault-bounded basin is a typical structural feature of the Basin and Range province (fig. 17); its marginal structures and basin-fill sediments control and host important hydrologic units throughout the region. Younger poorly-consolidated, finer-textured deposits consisting of interbedded pebbly, muddy sandstone and sandy pebble gravel form the dominant exposures in the main basin of Sonoita Creek. Fine and locally coarser materials (talus) generally are present in the active shoestring drainages within the upper canyons of the mountain ranges. In deep parts of the basin, sediments are typically medium-grained (pebble-cobble) sandy conglomerate with locally interbedded pebbly sandstones. This unit may be moderately consolidated at the base. Local cementation and red-staining of the alluvial deposits increases with proximity to the Patagonia fault zone and appears to represent iron-oxide-related diagenetic cementation. This cementation in its most extreme form produces ferricrete, that is, lenses of highly indurated iron-manganese-cemented conglomerate formed by the precipitation of iron from low pH waters derived from sulfide enriched source rocks. For example, terrace gravel along State Highway 82 near the mouth of Alum Canyon is irregularly impregnated with a black manganese-rich cement that contains anomalous amounts of base metals (Drewes, 1972b). Drewes (1972a) suggested that this material was probably introduced as a result of surface and ground waters that were laden with metals derived from mineralized terrane from the

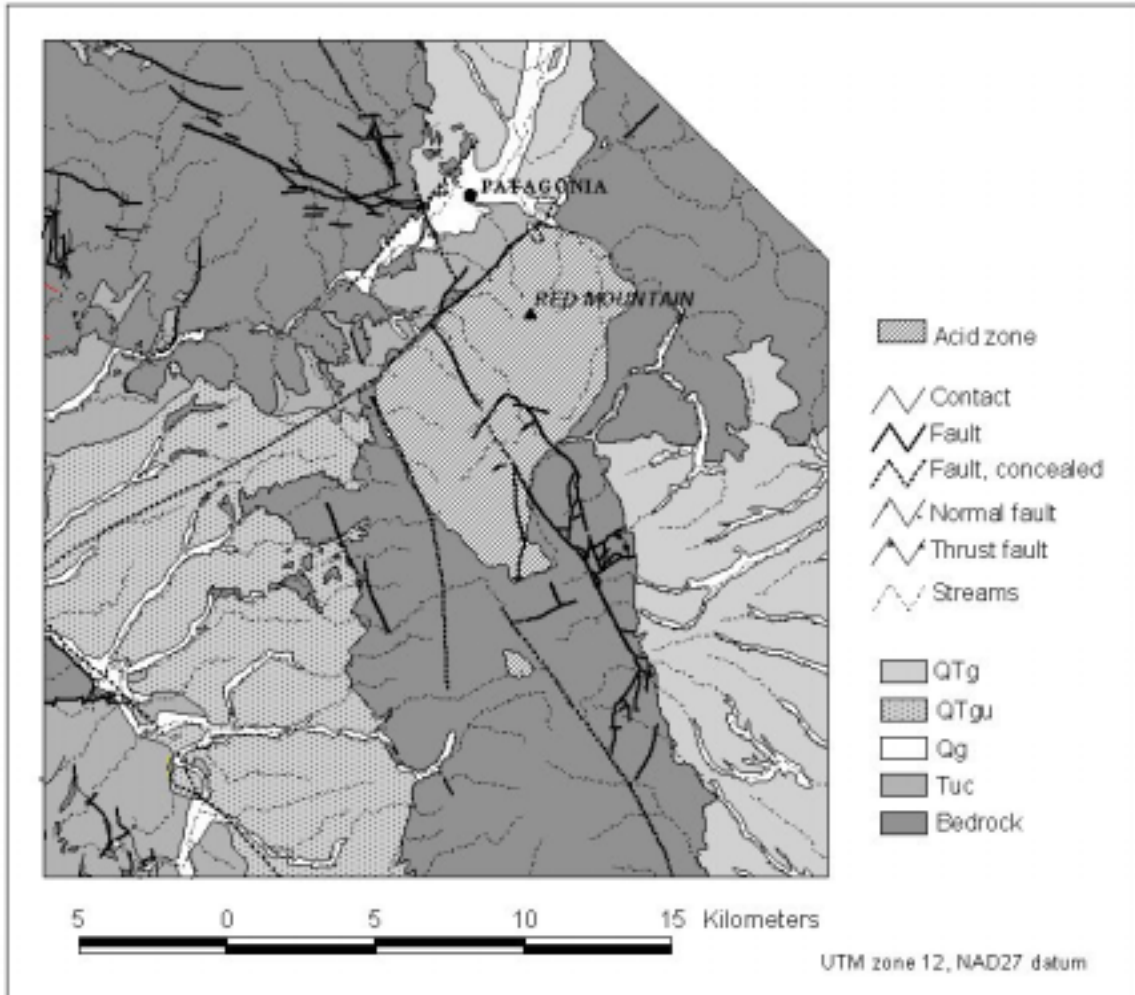


Figure 16. Bedrock-alluvium map illustrating the major lithologic units affecting groundwater transport and area outline of the extent of acid drainage in streams in the northern Patagonia Mountains area.

PRINCIPAL HYDROGEOLOGIC UNITS

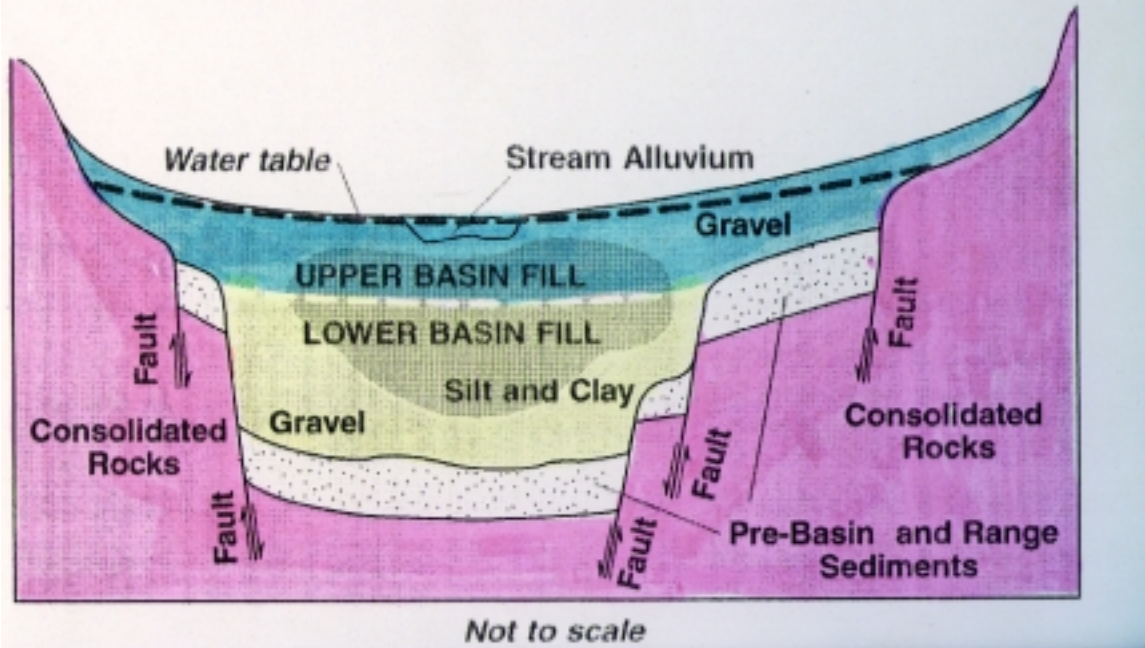


Figure 17. Sketch of principal hydrogeologic units within an idealized segment of the Basin and Range Province typical of the southwestern United States.

nearby bedrock from Red Mountain to the south, as is the present water emanating from Alum Canyon.

Overviews of region's hydrologic profile and initial results of SW Mineral and Environmental task 3

Fracture control is an important geologic feature of many ore deposits, not only in localizing hydrothermal fluids that transport and deposit mineral species but also in providing the principal modern conduits for local groundwater transport as discussed by Gray and others (1994) in their report on acid mine contamination at the Summitville Mine, Colorado. The interaction between surface and groundwater and sulfide-bearing rocks along permeable fracture sets creates acid water and water quality degradation is an important part of the environmental profile of the region. In the semi-arid climate of the southern Santa Rita and Patagonia Mountains, faults and fracture sets determine the siting of springs and seeps that are, in some cases, the source of limited perennial flow of creeks in the mountainous area. Approximately twenty-one predominantly ephemeral springs are located in the study area; all can be related to local faults or fracture systems. The largest cluster of springs exists just east of Temporal Gulch in the northern part of the area and is associated with the Santa Rita fault zone (fig. 16). The southernmost spring in this system is the unnamed spring at Sonoita Creek that provides some of the initial flow of the creek's perennial reach. Within Aztec Gulch (fig. 16) a spring located on a northeast-trending fault spur of the Patagonia fault provides perennial flow to a limited reach. Numerous silicified veins that record the paths of mineralizing thermal fluids found throughout the mountains are themselves the sites of seeps along their fractured margins. Humbolt canyon contains a cross section of veins with numerous mountainslope seeps that intersect the canyon. Limited ponded water can be found beneath these fractured areas within the adjacent streambed. Several adits emit effluent perennially or maintain standing water within the study area. Movement of water in near-surface fractures is virtually ubiquitous throughout the study area.

The quality of waters ranges from typical of southwest basin waters to degraded. Analyses of dissolved constituents show that there are two types of water in the study area: a calcium sulfate type and a calcium bicarbonate type. Another factor that establishes two broad groups of water is pH. One group of samples was found to cluster in a low pH range ($\text{pH} \leq 4.9$) and, another in a neutral to basic pH range (>6.9 to 8.7). Few samples were found in the 4.9 to 5.9 pH range. Those that fall into this range typically are derived from limestone bedrock. Figure 18, a plot of selected combined metals vs pH, shows the aforementioned separation of pH values and the relative values of combined metals from samples taken throughout the study area. When plotted on the diagram (modified from Plumlee and others, 1993) the waters cluster in the acid-high metals area and the near-neutral-low metals area. These diagrams are used to classify the effects of minerals deposits and their constituents on the surrounding aqueous environment.

To determine possible influences of mineralization and mining on the surface-water and ground-water systems, a comparison was made between the chemistry of waters collected in the Patagonia Mountains regions with average compositions of

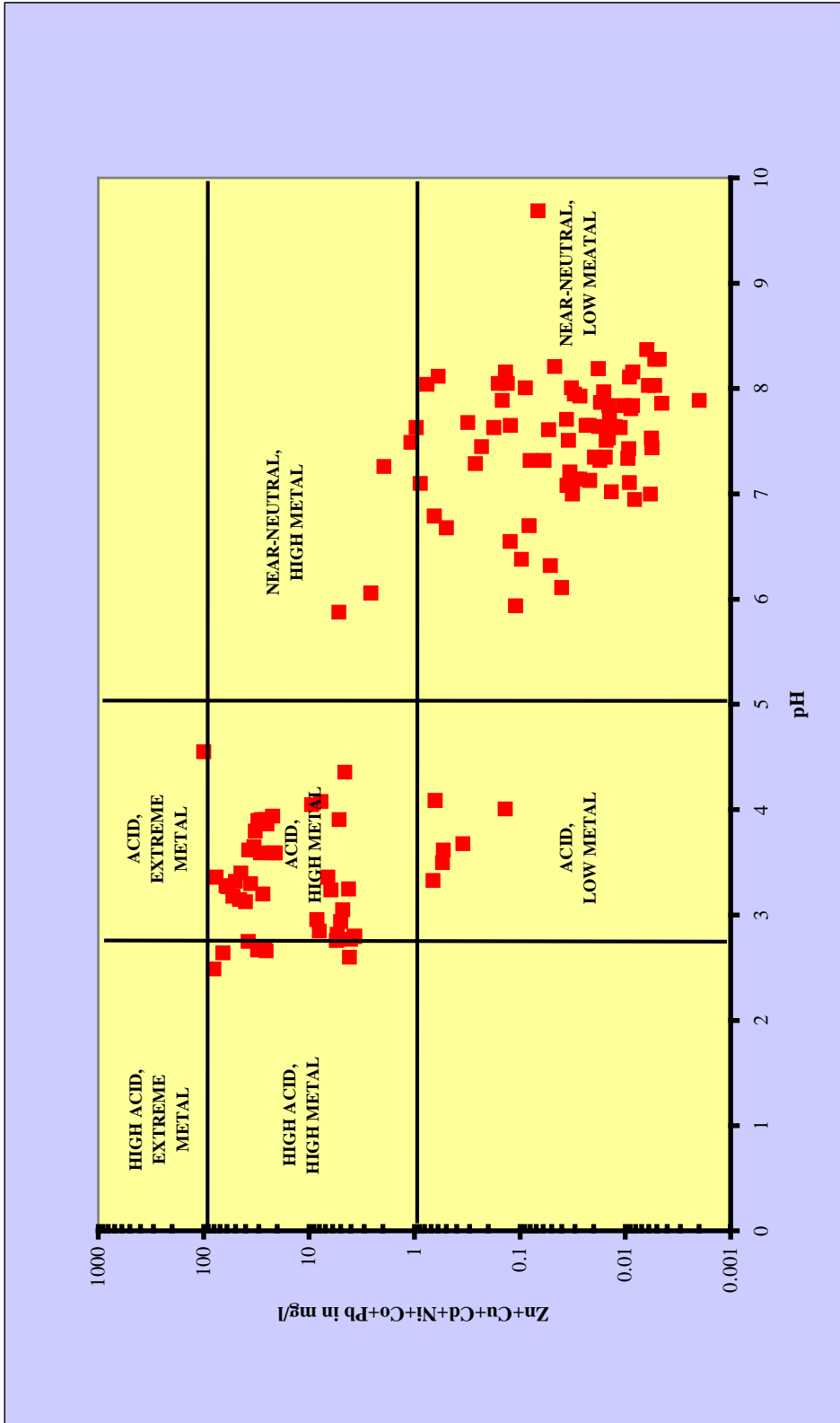
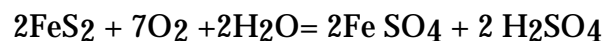


Figure 18. Variations in aqueous metal concentrations as a function of pH for all waters sampled in the study area. Classes for these waters are bounded by heavy lines and labeled with bold text (after Plumlee and others, 1993).

groundwater in basins of the semi-arid southwestern United States (Robertson, 1991). The ratio of selected metals concentrations in the variably mineralized study area to those found in the average southwestern U.S. basins is referred to as the enrichment factor.

Red Mountain (RM) and the smaller 4-Metals Mine area are sites of intense alteration and of at least two known porphyry copper deposits (RM) and an hydrothermal breccia pipe. The results of the comparison indicate that samples taken from drainages whose watersheds intersect the interior part of RM and the 4-Metals Mine area are significantly enriched in Al, Fe, Mn, Mg, Co, Cu, Pb, Zn, and SO₄. Of these elements, Al, Fe, Mn, Co, Cu, Zn show the highest enrichment (70-5,000 times), whereas Mg and Pb are less enriched (6 to 12 times). Na, K, Ca, As, Se, and U display only marginal enrichment values (1.3 to 3). Li, V, Sr, Mo, and Ba show depletion relative to the average of southwest basin waters. Enrichment factors of the anions SO₄, Cl, and F are 60, .8, and 75, respectively. Total dissolved solids in surface water and in groundwater wells are 1.9 times greater than average southwestern basin samples. The high values of sulfate and acid waters indicate surface and near surface oxidation of sulfides, mainly pyrite. Previous studies examining the water chemistry of selected drainages in the Patagonia Mountains have identified low pH and anomalous, metal-laden waters in primary 2nd order drainages emerging from the Red Mountain area and within minor interior drainages of the region (Dean, 1982; Dean and Fogel, 1982, Hyde, 1995). Geochemical studies of stream sediments from the region indicate anomalous metal values and confirm the potential for epithermal base and precious metals deposits.

The presence of elevated dissolved constituents in mineralized and mining influenced drainage begins with the breakdown of iron-bearing sulfide minerals (e.g. pyrite, chalcopyrite, sphalerite) present as disseminated minerals in the porphyry copper complex. Contributions of pyrite also occur when material piles (development rock) are disturbed and re-concentrated by mining activities. A common reaction for the oxidation of pyrite in the presence of atmospheric or dissolved oxygen is:



The water in contact with the minerals oxidized by the above reaction will be acidic and will contain high concentrations of sulfate (SO₄⁻²) and ferrous iron (Fe⁺²). The acid water accelerates the breakdown of clay, and other silicate minerals, thus increasing the concentrations of aluminum, calcium, magnesium, and manganese in mine waters.

Results from sampled areas outside of the Red Mountain mineralized zone, principally in Harshaw Creek, Temporal Gulch, and Sonoita Creek watersheds show much less pronounced enrichment. The fact that some level of enrichment is present is thought to be due to the proximity to the Red Mountain point source area. The picture that emerges is one of a prominent low-pH zone centered over the highlands of Red Mountain with an lower, outer zone of neutral to alkaline waters in alluvium and predominantly unaltered bedrock (fig. 16). The low volume of surface water coming

off the mountain flows into the alluvial skirt and enters the shallow groundwater system. Shallow wells in the alluvium less than 1 km from the point of entry of the acid water yield neutral water. The data indicate that the alluvial material at the margin of the basin is an effective chemical barrier or firewall, rapidly neutralizing the low pH waters as they flow downgradient in the aquifer and causing deposition of metals. During typical climatic conditions, this system is maintained during most of the year. However, elevated rainfall may generate enough surface runoff to bypass this buffering system and reach downstream sites that do not commonly receive low pH waters.

Other considerations

A number of converging and conflicting interests are present in the Patagonia-Santa Rita Mountains study area: (1) several of the mines located in the adjoining watersheds were identified in a list of high priority environmental degradation sites within the Coronado National Forest; as a result, the possibility that these sites may come under the Comprehensive Environmental Response Compensation and Liability Act of 1980 (CERCLA) needs to be evaluated; (2) there is doubt that some streams in the area associated with abandoned mine lands meet Arizona State water quality standards for clean water; (3) riparian waterway managers like the The Nature Conservancy (TNC) express concerns over future protection and maintenance of Sonoita Creek, a perennial stream; (4) the Town of Patagonia, upstream on Sonoita Creek from the riparian site, claims the right to use and expand use of water; and (5) local land owners do not understand the hydrogeologic basis of the geographic distribution of potable and unpotable groundwater in the area.

108.8 After lunch, continue to the southwest.

109.2 Join Az. Rt. 82 and continue southwest.

111.2 Turn south on Flux Canyon Road.

112.5 Turn left onto Aztec Gulch Road

114.1 Cross Aztec Creek, park vehicles, and walk 0.2 mi up unmaintained road to Aztec Mine

STOP 4 -- AZTEC GULCH: A look at geochemical baseline and background issues in the midst of widespread mineralization and after a century of underground mining.

This is the site of a low pH, metal-rich spring. We will consider (1) the geology of the area and its effect on the water chemistry, (2) the importance of considering this water as a component of storm runoff and its significance in remediation strategies, and (3) the geomorphology of the canyon and iron deposition (ferricrete) in the valley.

The spring in Aztec Gulch is in a fracture zone located on the margin of the porphyry copper body at Red Mountain (fig. 16). Oxidized, copper stained stockwork veins are present in a cut in the canyon wall just above the spring site. Although only rare sulfide minerals can be seen at the surface, information from drilling indicates that

sulfide minerals are present in abundance at shallow depth. The low pH and high iron content of the water emerging from the fracture zone indicate it has reacted with sulfide-bearing rock in the aquifer. These highland “resident” waters of an area reflect the geoenvironmental conditions in the vicinity of a mineralized system, but as mentioned earlier, these waters do not typically reach the lower parts of the drainage except during episodes of rapid runoff following storms. During these rapid runoff events, low pH surface waters are an important component of the chemical aspect of total runoff in the lower parts of the drainage.

A Simulated Rainfall Study (SRS) was devised to properly answer client concerns about storm runoff. The SRS is an attempt to understand the chemistry of rainwater interaction with the major material components that make up the watershed. Dionized water will be washed over various outcrops, tailings and waste rock piles, analyzed and subsequently modeled and compared to actual storm runoff samples. Resident water, i.e., water that is part of the groundwater system of the region, emerges from springs, adits, and seeps, displays variable chemistry, and is commonly misinterpreted as the major or only component of storm runoff. However, mean values of dissolved metals in waters found in adits and associated with waste rock may be more than an order of magnitude greater than natural background samples from seeps, springs and deep exploration wells within the mineralized zone.

The part of Aztec Canyon visible from here has undergone substantial erosion during the Tertiary and Quaternary. Mass wasting and debris flow deposition is evidenced in the walls of the canyon. The rich iron staining present as intergranular cement and coatings on the outcrops suggests a long history of circulating iron-rich water was involved in the weathering of parts of this alluvial deposit.

On the way down we'll point at the extension of the Santa Rita fault zone (fig. 16) and view this example of ferricrete formation and its implications for limited contaminant transport (information gathered here is pertinent to Stop 5).

114.1 Return to cars and retrace route to Az. Rt. 82.

116.0 Turn right on Az. Rt. 82, back toward Patagonia.

118.4 Turn left on 4th Ave.

118.5 Turn left on Pennsylvania Ave.

118.7 Cross-Sonoita Creek -- usually dry here.

119.3 Spring at beginning of perennial flow in Sonoita Creek

**STOP 5 -- SONOITA CREEK AT THE NATURE CONSERVANCY PRESERVE:
spring flow beginnings of riparian reach of creek**

The Nature Conservancy's Patagonia-Sonoita Creek Preserve (fig. 16) protects one of the most lush riparian communities in southern Arizona. The Preserve features the perennial flow reach of Sonoita Creek and the diverse habitat existing along the

banks of the creek. The main objectives of this stop are to review evidence for (1) a fault controlled source for the creek water, (2) the complexities of source water for surface flows; and (3) runoff effects on the stream during storm episodes.

Following the path of the birdwatchers, we look down instead of up. By integrating data of this project with those of an ADWR-funded study, we present a concept of multiple sources for the emergence of flow in Sonoita Creek and gather evidence for leakage through the alluvial firewall. The perennial reach of Sonoita Creek begins below Patagonia, Arizona and flows 8 km to Patagonia Lake (fig. 16), providing a case study of the complex hydrologic conditions existing in desert riparian systems. This reach is supplied by groundwater inflow from three sources, as evidenced by geo-hydrologic, geophysical, and water-quality information. Groundwater movement along the Santa Rita fault plane (fig. 16) provides the initial stream source. This source has a negligible flow rate and a pH of 5.5, unlike that of water from adjacent and upstream aquifers. The second source of inflow enters as a large (4 cfs) influx about 1.5 km downstream and is derived from a plume of ground-water believed to be related to Temporal Gulch (fig. 16). A third influx enters near Solero Canyon (fig. 16) to the west, producing a gradual increase in flow rate (2 cfs). The initial spring flow along the Santa Rita fault is the main source of elevated sulfate and metal values from mineralized bedrock immediately beneath the spring and to the south.

Intense rains produce rare, high-volume storm run-off events causing the acid-bearing streams of Red Mountain to reach Sonoita Creek. Therefore, episodic acidic, metal-laden floodwaters have affected the creek on a near annual basis, probably throughout the Holocene, and may have been a restricting parameter for the diversity of fauna and flora of the riparian area. Future studies will be aimed at determining the extent, intensity, and timing of these episodic events downstream in the sediments deposited in Patagonia lake. Figure 19 shows the variable load of selected metals in Sonoita Creek during normal flow periods and during an elevated flow period when acidic waters from Red Mountain to the south flowed down Flux Canyon and mixed with water in Sonoita Creek.

We will continue on down the graded road to where the creek has considerably greater discharge.

119.3 Continue southwest on graded road.

120.0 The Nature Conservancy visitor center is on the left. There are restrooms at the visitor center. This brief stop serves to point out some aspects of the structural setting of the basin and the geologic controls on the water quality within the basin.

Although the Conservancy's Preserve contains a healthy riparian reach of good quality surface water, the main supply well, located in bedrock near the road, yields water with a surprisingly low pH of 4.6. Look at the bedrock near the caretaker's house on the right for a possible answer. The light colored rock with yellowish-brown to reddish-brown staining indicates the rock has been altered (from the breakdown of sulfides) and probably has little or no buffering capacity. Porewaters within the fractured rock are acidic and the well is placed to utilize the bedrock aquifer. A new well, drilled near the visitor center less than 100 m to the south, yields slightly alkaline water with a pH of 7.9-8.2. Geophysical studies, conducted by the University of

SONOITA CREEK CREEK SAMPLES

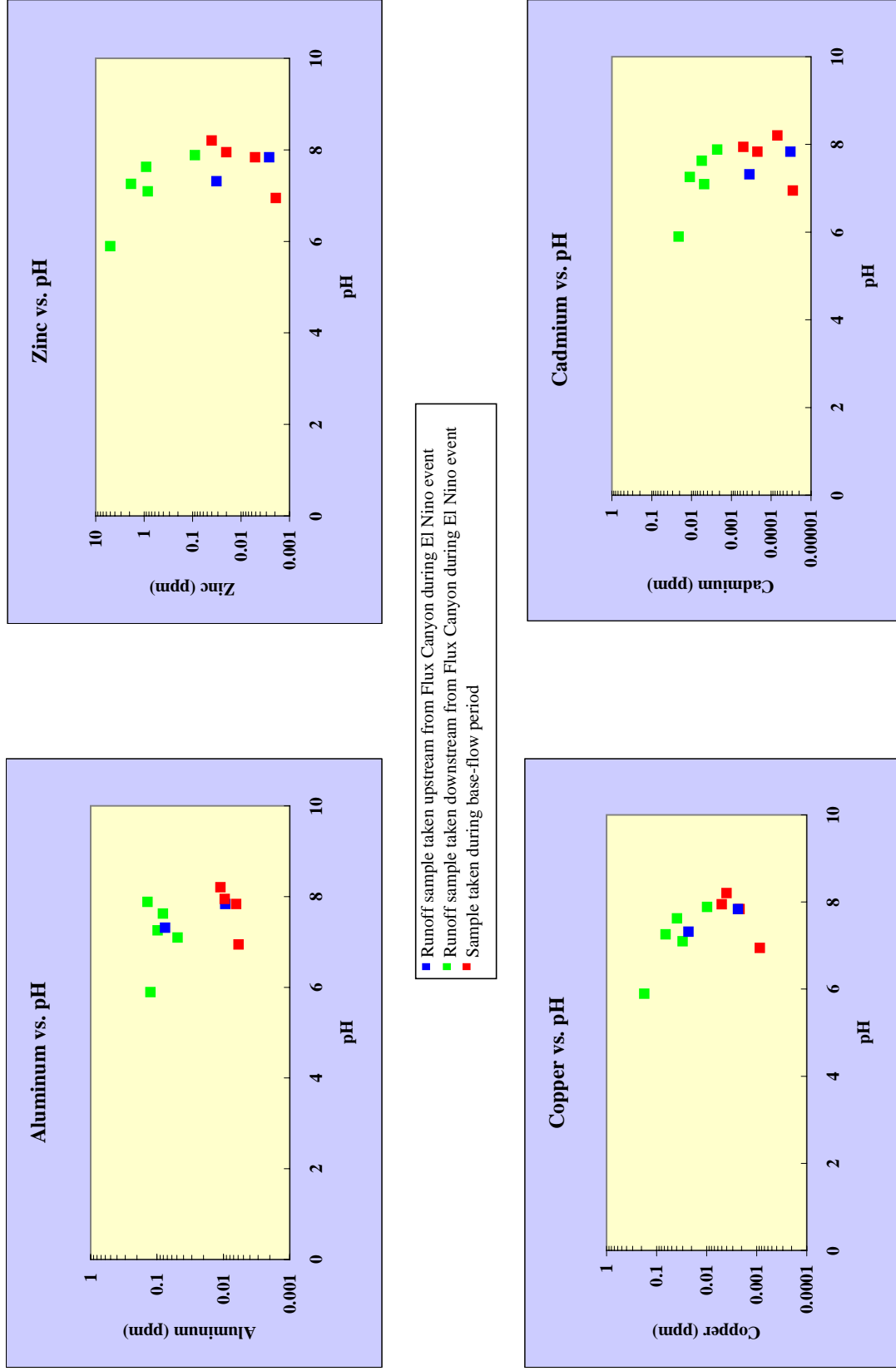


Figure 19. Plots of storm water (elevated) type episodic event showing contaminate influence.

Arizona Department of Hydrology in cooperation with this project, indicate a very steep drop in the basin's bedrock floor between the road and the visitor center. The basin fill underneath the center may be as thick as 300 m. The thick basin-fill alluvium effectively buffers all acidic waters passing into it from the bedrock.

121.5 Road junction; turn left

121.6 Cross Sonoita Creek.

121.9 Turn right onto Az. Rt. 82.

126.0 Patagonia Lake State Park is on the right. Overview of Nogales, Sonora and Nogales, Arizona is to the southwest (figs. 1 and 2).

129.5 Nogales International Airport is on the left. Patagonia Mountains are to the east and Sierra San Antonio (in Sonora) is to the southeast

131.5 From here, on through Nogales and north on I-19 to about mile 139.4, there are many excellent exposures of a number of different facies of the Nogales Formation, which is the indurated lower conglomerate unit in the upper Santa Cruz basin.. Two age dates for the Nogales Formation have been obtained from interbedded volcanic units in Agua Fria Canyon, about 9 mi northwest of Nogales. Simons (1974) reported a whole-rock K-Ar date of 12.6 Ma on a spinel-bearing basalt flow interbedded near the base of the formation. Sanidine in pumice from a basal ash-flow tuff yielded an $^{40}\text{Ar}/^{39}\text{Ar}$ date of 13.23 ± 0.10 Ma (Houser, unpublished data).

132.0 Cross the Santa Cruz River (dry). Nogales, Arizona municipal pumping plant on the right

136.2 Turn left at the light on Grand Ave.

137.3 Turn left at the light onto Az. Rt. 189.

137.8 Note exposure of Nogales Formation behind the shopping center on the left.

138.0 Turn right onto I-19 north. Good exposures of the Nogales Formation in road cuts.

141.7 From here on north, exposures in road cuts are Pliocene basin-fill alluvium and Quaternary surficial materials. This exposure is representative of the poorly indurated upper basin-fill sedimentary unit of the upper Santa Cruz basin.

145.8 San Cayetano Mountains are on the east (figs. 1 and 2).

153.1 Tumacacori Mountains are on the west; Mount Hopkins and Smithsonian observatory are on the east.

Tumacacori Mountains and Mount Benedict fault

The Tumacacori mission on the east was one of the Jesuit missions established by Fr. Kino in 1697. The present church was built in about 1800 and abandoned by about 1840 because of Apache raids.

The Mt. Benedict fault, shown on figures 1, 20, and 21, crosses the road from southeast to northwest just north of here. The linear magnetic low on figure 21 defines the fault zone northeast of Mt. Benedict.

The Tumacacori Mountains are underlain by Oligocene rhyolite that may be outflow ash-flow tuff sheets in part. Although no source has been identified for them, Drewes (1996) suggested that a volcanic eruptive center in the Grosvenor Hills southwest of the Santa Rita Mountains may have been a source. Along the west side and north end of the Tumacacori Mountains, the volcanic rocks form a thin cap on a basement of Mesozoic volcanic and plutonic rocks, some of which are mineralized (Drewes, 1996).

163.1 Elephant Head (fig. 2) in the Santa Rita Mountains to the east.

166.0 Rest area and Stop 6.

STOP 6 -- AEROMAGNETIC SURVEY: Santa Cruz Valley subbasins; data for a mineralized area on the west side of the Santa Rita Mountains

Santa Cruz Valley and western Santa Rita Mountains

This stop provides an overview of the upper Santa Cruz Valley and the bordering Santa Rita Mountains to the east (fig. 2). Though the valley is physiographically a large single basin, as is the case in the San Pedro Valley, once again the gravity-anomaly data show that, between here and Nogales, there are four subbasins with intervening bedrock highs (Gettings and Houser, 1997) (fig. 20). Houser has shown that the bedrock highs still influence the surficial deposits in that the gradient of the Santa Cruz River increases over each high (fig. 20). The analysis of the gravity-anomaly data for this area was requested and partly funded by the Arizona Department of Water Resources. It was this study that produced the technique of mapping the contact between unconsolidated and consolidated basin fill that has been used in this and the San Pedro tasks.

The upper Santa Cruz basin is filled mostly with conglomerate of the Miocene Nogales Formation, which is moderately to well consolidated and a poor aquifer. The volume of younger unconsolidated basin fill is quite small; the largest amount is in the Amado subbasin, which we are now looking across to the east.

The Solero mining district is at the foot of the western slope of the Santa Rita Mountains in the Cottonwood Canyon area (fig. 2). The district contains at least three deposits mined for lead and silver by the Spanish working out of the mission at Tumacacori; the Glove, the Montosa and the Solero Mines (Drewes, 1996). These deposits are the quartz-carbonate vein type. As a result of our critique of the quantitative assessment methods, we were led to examine a new technique of quantifying the possibility of the occurrence of a deposit of given type using fuzzy logic

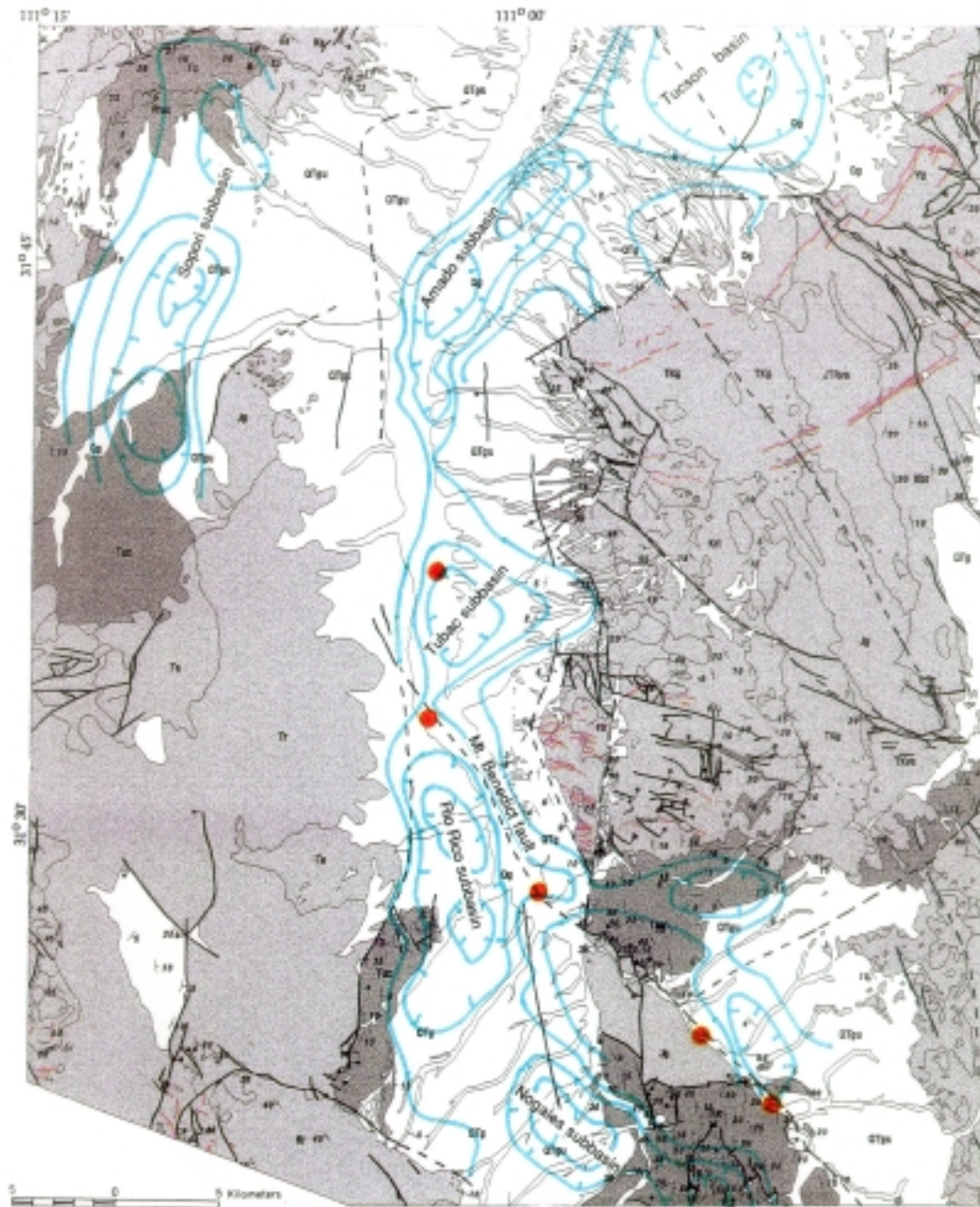


Figure 20 Generalized geologic map of the upper Santa Cruz Valley showing approximate location of subbasins based on complete Bouguer gravity anomaly map. Gravity contour interval is schematic. Light shaded units are prebasin-fill rock; dark shaded unit is Nogales Formation; unshaded areas are upper basin fill and Quaternary alluvium. Orange dots indicate reaches of significantly higher gradient in the Santa Cruz river. Geology compiled by Dewes (1980) and modified by Houser (unpublished data).

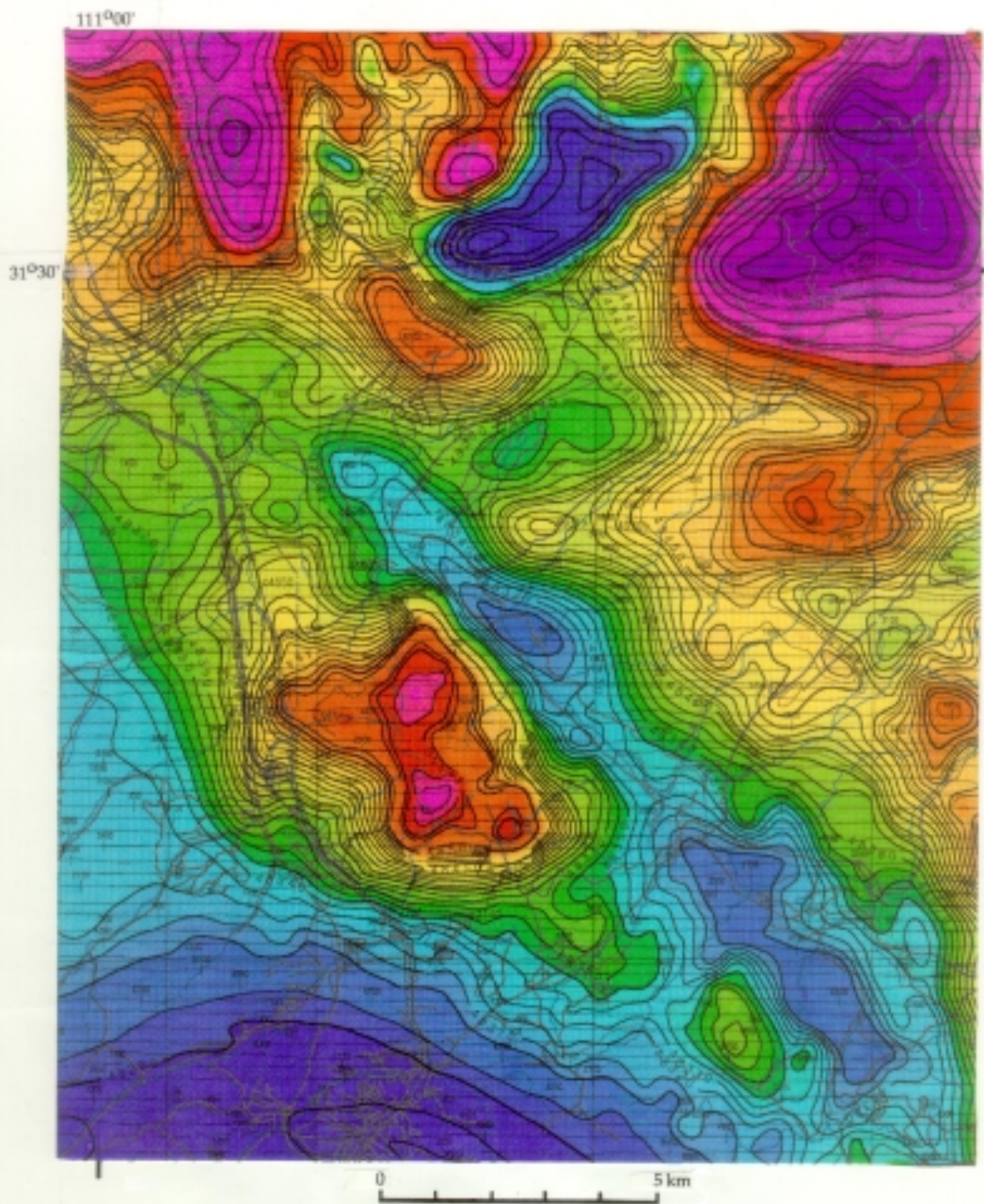


Figure 21. Aeromagnetic map of the Mt. Benedict area showing narrow half graben to the east along the Mt. Benedict fault. Red colors are relative magnetic highs: blue colors are relative magnetic lows. Compare with figure 1 for location of roads and streams

(Gettings and Bultman, 1993). This worked so well for the area of exposed rock that we decided to expand the area to include shallowly buried bedrock immediately west of the range front. Aeromagnetic and airborne electromagnetic data have been flown over the area (1998) and we are currently working on a district study for this deposit type combined with prospecting for buried targets which may be new ore bodies.

In 1996, detailed (250 m line spacing) aeromagnetic data were flown over the valley and bounding ranges. One of the results is that a number of faults scarps in the Pleistocene surficial materials are seen to have magnetic anomalies. Modeling the gravity and magnetic effects of these faults and finding the relation between the faults in the basin fill, the fault in bedrock, and the geophysical signatures of the fault is the subject of an M.S. thesis being carried out by Chris Baldyga of the University of Arizona Department of Hydrology with USGS support.

Airborne electromagnetic data were also obtained in two areas to the south (Tubac and Nogales subbasins) and in a large area from Green Valley to the Santa Rita Mountains in the Huerfano Butte area (fig. 2). Surveys in the southern areas were carried out mainly for water table mapping purposes while the Huerfano Butte area was flown to look for possible mineral deposits on the bedrock high between the Amado subbasin and the Tucson basin to the north. Additionally, detailed aeromagnetic data of the Tucson basin were acquired last year. We now have more data than we have staff to interpret it. We have allocated money to support two new Master's students to do theses on the interpretation of parts of these data.

172.4 Tailings on the west behind Green Valley (fig. 2) are from the Twin Buttes Mine and ASARCO's Pima-Mission Mine. Pfizer marble quarry is to the east across the Santa Cruz Valley on the west side of Mt. Fagan.

178.3 Overview of Tucson basin, and the Santa Catalina and Rincon Mountains. Pecan groves in the valley in the Santa Cruz flood plain are watered by large irrigation wells.

184.9 Black Mountain lies to the northwest (fig. 2).

187.7 Towers of the San Xavier del Bac Mission can be seen a couple miles to the west; Tucson Mountains in the background (fig. 2).

186.5 Cross the Santa Cruz River; Martinez Hill on the right consists of Tertiary andesite flows and interbedded tuff and volcanoclastics.

196.9 Exit I-10 at St. Mary's Road and go east.

198.5 Arrive back at ENRB at 6th St. and Park Ave.

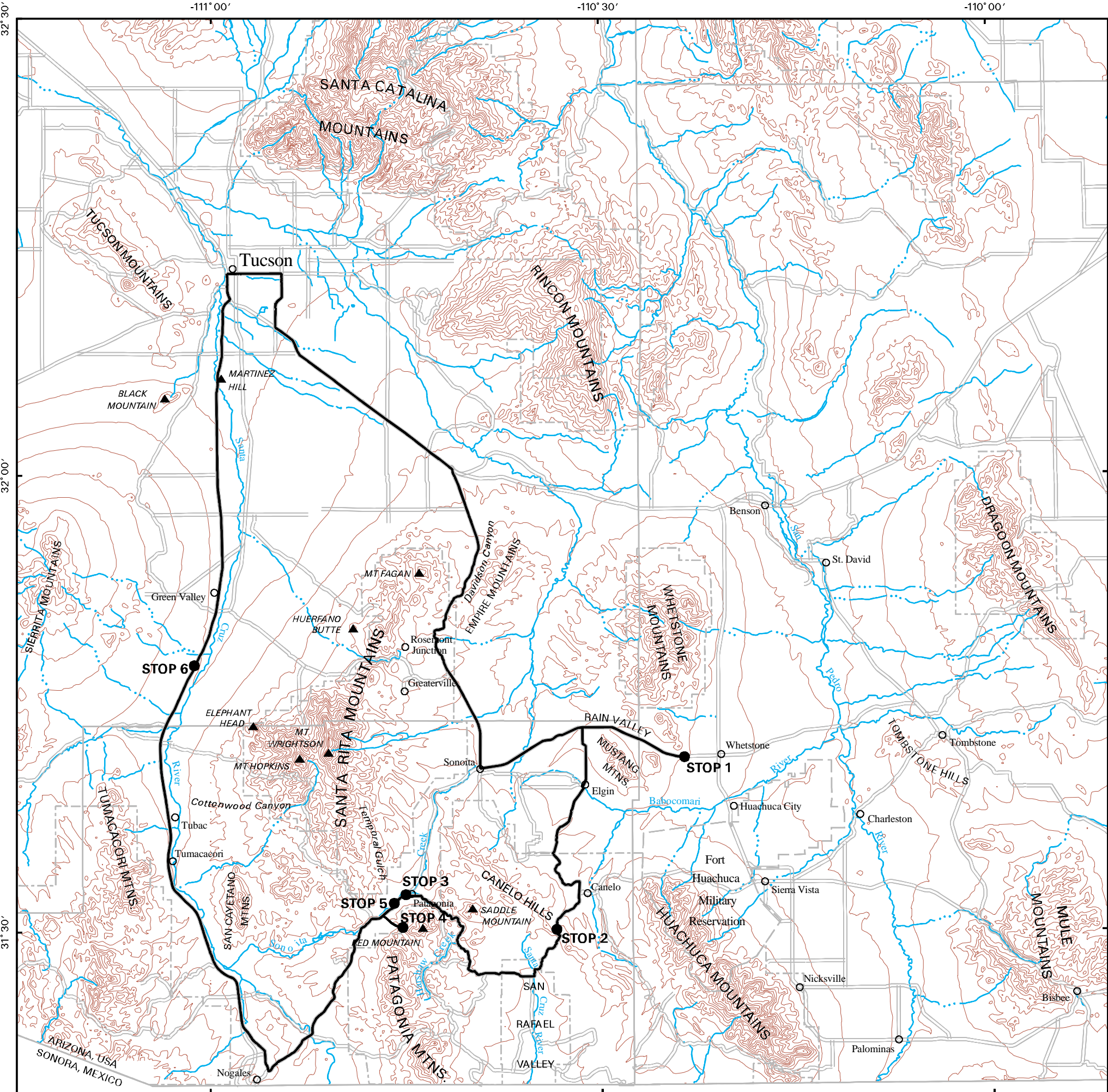
REFERENCES CITED

- Bultman, M.W., Gettings, M.E., and Wynn, J.C., 1999, An interpretation of the 1997 Airborne ElectroMagnetic (AEM) survey, Fort Huachuca vicinity, Cochise County, Arizona: U.S. Geological Survey Open-File Report 99-7-A, CD-ROM.
- Corn, R.M., 1975, Alteration-mineral zoning, Red Mountain, Arizona: *Economic Geology*, v. 70, p. 1437-1447.
- Cox, L.J., 1992, Geology of the gold placers in the Greaterville district, Arizona, in Houser, B.B., comp., *Historic mining camps and Jurassic calderas: Tucson, Arizona Geological Society Guidebook, Fall field trip, 1992*, p. 36-46.
- Dean, S.A., 1982, Acid drainage from abandoned metal mines in the Patagonia Mountains of southern Arizona, Coronado National Forest: USDA Forest Service.
- Dean, S.A., and Fogel, M.M., 1982, Acid drainage from Abandoned metal mines in the mountains of southern Arizona: *Symposium on Surface Mining, Hydrology, Sedimentology, and Reclamation, December 5-10, 1982, Proceedings*, p. 269-277.
- Dickinson, W.R., 1991, Tectonic setting of faulted Tertiary strata associated with the Catalina core complex in southern Arizona: *Geological Society of America Special Paper 264*, 106 p.
- Drewes, H.D., 1971a, Geologic map of the Mount Wrightson Quadrangle, southeast of Tucson, Santa Cruz and Pima Counties, Arizona: U.S. Geological Survey Miscellaneous Investigations Series Map I-614, scale 1:48,000.
- _____, 1971b, Mesozoic stratigraphy of the Santa Rita Mountains, southeast of Tucson, Arizona: U.S. Geol. Survey Professional Paper 658-C., 81 p.
- _____, 1972a, Cenozoic rocks of the Santa Rita Mountains, southeast of Tucson, Arizona: U.S. Geological Survey Professional Paper 746, 66 p.
- _____, 1972b, Structural geology of the Santa Rita Mountains, southeast of Tucson, Arizona: U.S. Geological Survey Professional Paper 748, 35 p.
- Drewes, H.D., 1980, Tectonic map of southeast Arizona: U.S. Geological Survey Miscellaneous Investigations Series Map I-1109, scale 1:125,000.
- Drewes, H.D., 1981, Tectonics of southeastern Arizona: U.S. Geological Survey Professional Paper 1144, 96 p.
- Drewes, H. D., 1996, Geology of Coronado National Forest, Chapter B, in duBray, E. A., ed., *Mineral Resource Potential and Geology of Coronado National Forest, Arizona and New Mexico*: U.S. Geological Survey Bulletin 2083-B, pp 19-41.
- Finnell, T.L., 1974, Preliminary geologic map of the Empire Mountains quadrangle, Pima County, Arizona: U.S. Geological Survey Open-File Report 1971, scale 1:48,000.
- Gettings, M.E., and Bultman, M.W., 1993, Quantifying favorableness for occurrence of a mineral deposit type using fuzzy logic - an example from Arizona: U.S. Geological Survey Open-File Report 93-392, 13 p.
- Gettings, P.E. and Gettings, M.E., 1996. Modeling of a magnetic and gravity anomaly profile from the Dragoon Mountains to Sierra Vista, southeastern Arizona: U.S. Geological Survey Open File Report 96-288, 13 p.
- Gettings, M.E., and Houser, B.B., 1997, Basin geology of the upper Santa Cruz Valley, Pima and Santa Cruz Counties, southeastern Arizona: U.S. Geological Survey Open File Report 97-676, 40 p.

- Gettings, M.E. and Houser, B.B., 1999, Depth to bedrock of the upper San Pedro Valley, Cochise County, southeastern Arizona: U.S. geological Survey Open-File Report, in preparation, 34 p.
- Granger, B.H., 1960, Will C. Barnes' Arizona Place Names: Tucson, University of Arizona Press, 519 p.
- Gray, John E., Coolbaugh, Mark F., Plumlee, Geoffrey S., and Atkinson, William W., 1994, Environmental geology of the Summitville Mine, Colorado: Economic Geology, vol. 89, 1994, p. 2006-2014.
- Gray, Floyd, Chaffee, M.A., Wirt, Laurie, Lichte, F.E., and Caruthers, Kerry, 1997, Source chemistry and characteristics of intermittent stream waters having low pH and elevated metal concentrations, Patagonia Mountains, Santa Cruz County, Arizona *in* Wanty, R.B., Marsh, S.P., and Gough, L.P., eds, 4th International Symposium on Environmental Geochemistry, Program with Abstracts, U.S. Geological Survey Open File Report 97-496, p 30-31.
- Gray, Floyd, Wirt, Laurie, Caruthers, Kerry, Bolm, K.S., and Chaffee, M.A., 1998, Source chemistry and characteristics of stream waters having low pH and elevated metal concentrations, Patagonia and southern Santa Rita Mountains, Santa Cruz County, Arizona-- Implications for impacts into Sonoita Creek and upper Santa Cruz River basin, *in* Gottfried, G.J., Edminster, C.B., and Dillon, M.C. comps., Cross border waters -- fragile treasures for the 21st century: Ninth US/Mexico Border States Conference on Recreation, Parks, and Wildlife: Proceedings RMRS-P-5: US Department of Agriculture, Forest Service, Rocky Mountain Research Station, 341 p.
- Graybeal, F.T., 1973, Copper, manganese, and zinc in coexisting mafic minerals from Laramide intrusive rocks in Arizona: Economic Geology, v. 68, p. 785-798.
- Graybeal, F.T., 1984, Metal zoning in the Patagonia Mountains, Arizona, *in* Wilkins, Joe, Jr., ed., Gold and Silver Deposits of the Basin and Range Province, Western USA: Tucson, Arizona Geological Society Digest, v. 15, p. 187-197.
- _____, 1996, Sunnyside -- A vertically preserved porphyry copper system, Patagonia Mountains, Arizona: Society of Economic Geologists Newsletter, no. 26, p. 9-14.
- Hayes, P.T., and Raup, R.B., 1968, Geologic map of the Huachuca and Mustang Mountains, southeastern Arizona: U.S. Geological Survey Miscellaneous Investigations Series Map I-509, scale 1:48,000.
- Haynes, C.V., Jr., 1987, Curry Draw, Cochise County, Arizona -- A late Quaternary stratigraphic record of Pleistocene extinction and paleo-Indian activities: Geological Society of America Centennial Field Guide, Cordilleran Section, p. 23-28.
- Houser, B.B. and Gettings, M.E., 2000, Stratigraphy and tectonic history of the Tucson basin, based on re-examination of cuttings and geophysical logs of the Exxon State (32)-1 well: U.S. Geological Survey Open-File Report 00-139, 38 p.
- Hyde, Peter, 1995, Water quality at the Trench Camp, Patagonia Mountains, Santa Cruz County, Arizona April 3-4, 1995: Arizona Department of Environmental Quality Report, Aquifer Protection Section, 15 p.
- Koutz, F.R., 1984, the Hardshell silver, base metal, manganese oxide deposit, Patagonia Mountains, Santa Cruz County, Arizona -- A field trip guide, *in* Wilkins, Joe, Jr.,

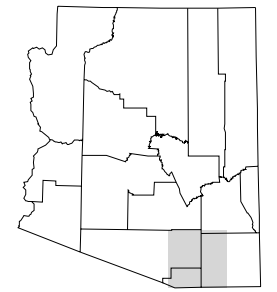
- ed., *Gold and Silver Deposits of the Basin and Range Province, Western USA: Tucson, Arizona Geological Society Digest*, v. 15, p. 199-217.
- Lehman, N.E., 1978, *The geology and pyrometasomatic ore deposits of the Washington Camp-Duquesne district, Santa Cruz County, Arizona: Tucson, University of Arizona*, Ph.D. dissertation, 285 p.
- Lipman, P.W., and Hagstrum, J.T., 1992, *Jurassic ash-flow sheets, calderas, and related intrusions of the Cordilleran volcanic arc in southeastern Arizona - Implications for regional tectonics and ore deposits: Geological Society of America Bulletin*, v. 104, p. 32-39.
- Macnae, J.C., Smith, Richard, Polzer, B.D., Lamontagne, Y., and Klinkert, P.S., 1991, *Conductivity-depth imaging of airborne electromagnetic step-response data: Geophysics*, vol. 56. no. 1, p. 102-114.
- Moore, R.B., 1993, *Geologic map of the Tombstone volcanic center, Cochise County, Arizona: U.S. Geological Survey Miscellaneous Investigations Series Map I-2420*, 1 sheet, scale 1:50,000.
- Plumlee, G.S. Smith, S.M., Toth, M.I., and Marsh, S.P., 1993, *Integrated mineral-resource and mineral-environmental assessments of Public Lands: Applications for Land Management and Resource Planning, U.S. Geological Survey Open-File Report 93-571*.
- Quinlan, J.L., 1986, *Geology and silicate-alteration zoning at the Red Mountain porphyry copper deposit, Santa Cruz County, Arizona, in Beatty, Barbara, and Wilkinson, P.A.K., eds., Frontiers in geology and ore deposits of Arizona and the southwest: Tucson, Arizona Geological Society Digest Volume 16*, p. 294-304.
- Riggs, N.R., and Busby-Spera, C.J., 1990, *Evolution of a multi-vent volcanic complex within a subsiding arc graben depression - Mount Wrightson Formation, Arizona: Geological Society of America Bulletin*, v. 102, p. 1114-1135.
- Robertson, F.N., 1991, *Geochemistry of ground water in alluvial basins of Arizona and adjacent parts of Nevada, New Mexico, and California: US Geological Survey Professional Paper 1406-C*, 90 p.
- Schrader, F.C., 1915, *Mineral deposits of the Santa Rita and Patagonia Mountains, Arizona: U.S. Geological Survey Bulletin 582*, 373 p.
- Schafroth, D.W., *Structure and Stratigraphy of the Cretaceous rocks south of the Empire Mountains, Pima and Santa Cruz Counties, Arizona: Tucson, University of Arizona Ph.D. dissertation*, 135 p.
- Sherman, J.E., and Sherman, B.H., 1969, *Ghost Towns of Arizona: Norman, University of Oklahoma Press*, 208 p.
- Simons, F.S., 1972, *Mesozoic stratigraphy of the Patagonia Mountains and adjoining areas, Santa Cruz County, Arizona: U.S. Geological Survey Professional Paper 658-E*, 23 p.
- _____, 1974, *Geologic map and sections of the Nogales and Lochiel quadrangles, Santa Cruz County, Arizona: U.S. Geological Survey Miscellaneous Investigations Series Map I-762*, scale 1:48,000.
- Tatlow, M., 1998, *San Pedro Model area well information from GWSI database: written communication, Arizona State Department of Water Resources*, 12 p., 652 well measurements.

Tenney, J.B., 1929, History of mining in Arizona: Tucson, University of Arizona Library, Special Collections, unpublished manuscript, 401 p.
Wagoner, J.J., 1975, Early Arizona - Prehistory to Civil War: Tucson, The University of Arizona Press, 547 p.



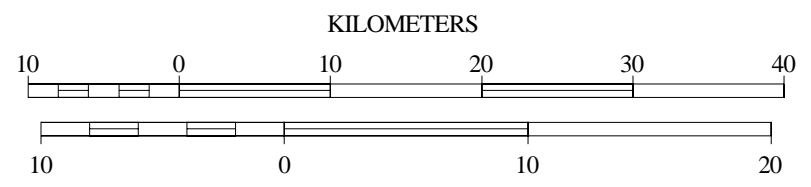
Field Trip Route and Stops

- Trip Route
- Streams
- Roads
- National Forest Boundaries
- Military Reservation Boundary
- County, State, International Boundaries
- Field Trip Stop
- Peak
- Town



MAP LOCATION

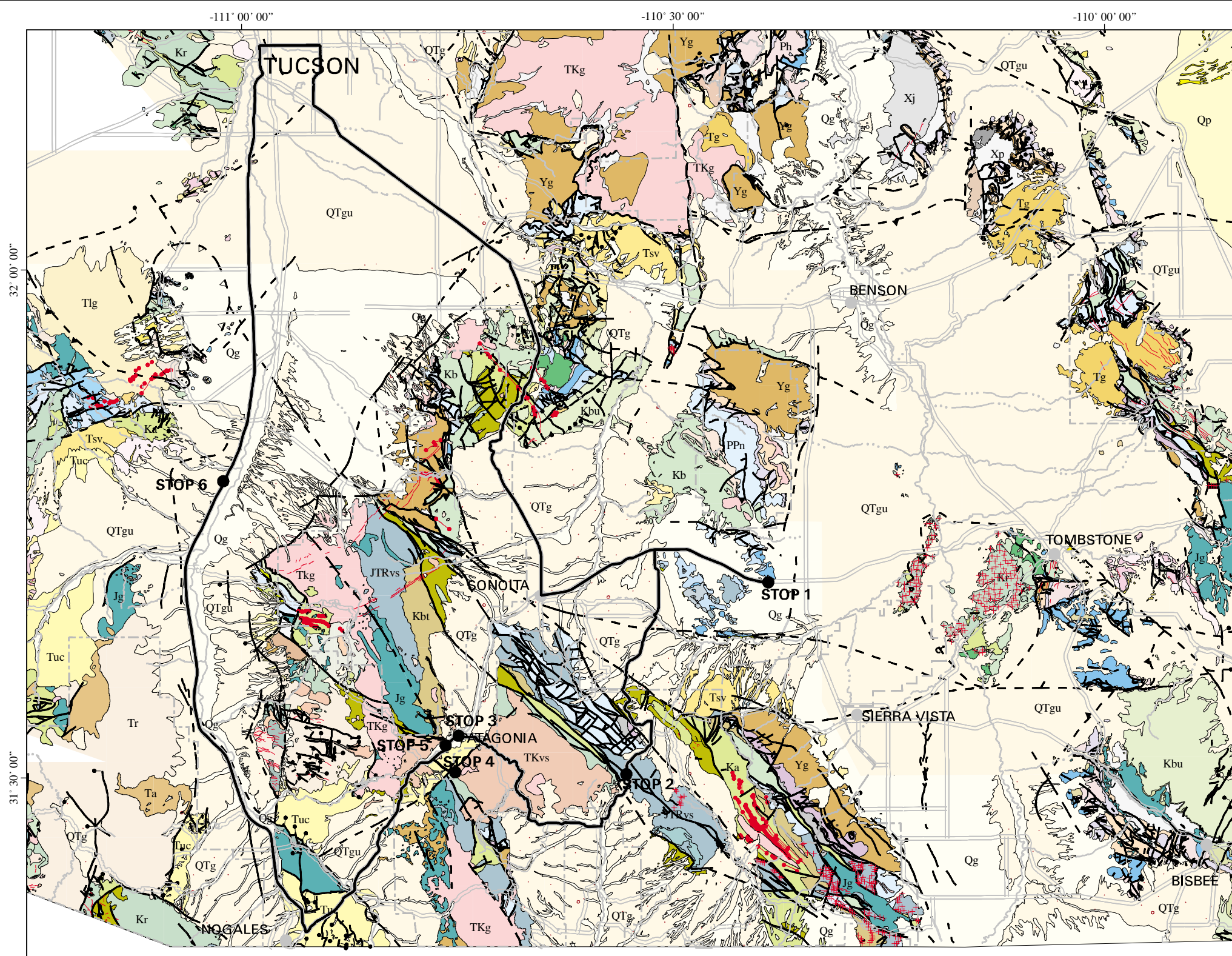
Contour interval 100 meters



MILES

UTM zone 12, NAD27 Datum

Figure 2. Map of part of southeastern Arizona showing field trip route and geographic features mentioned in the text.

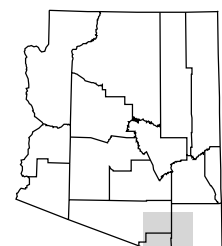


KEY (Descriptions on following page)

Qg	Tv	Ksv	JTri	Yd
Qd	Tug	Kus	JTRvs	Ya
Qp	Ti	Kr	TRm	Yg
QTg	Ta	Krt	TRs	Yw
QTgu	Tlc	Ka	TRvs	Yr
QTb	Tlp	Klq	PzYm	Yc
Tuc	Tlv	Ks	Pzs	Yt
Tb	Tlg	Ki	PPn	YXm
Tc	TKg	Kb	Ps	Xj
Tsv	TKvs	Kbu	PPs	Xp
Tr	TKa	Kbg	Ph	Xi
Trt	TKr	Kbt	Ms	
Tri	TKp	Klvs	MDs	
Tg	Kd	Jg	Pzl	
Tva	Kq	Jr	Cs	

- CONTACT-Dotted where concealed, queried where uncertain
- FAULT-Showing dip; dotted where concealed or intruded, queried where uncertain. Where solid line becomes dotted line within a map unit, that unit is a composite of several formations, of which a younger one conceals faulting in an older one.
- NORMAL FAULT-Ball and bar on downthrown side; dotted where concealed, queried where uncertain.
- THRUST FAULT-Sawteeth on upper plate.
- GLIDE FAULT-Open sawteeth on glide plate.
- DIKES- Tri
- DIKES-Ti
- DIKES- TKr
- DIKES-TKp
- DIKES- Yd

GEOLOGIC MAP OF SOUTHEASTERN ARIZONA



MAPLOCATION



UTM Zone 12, NAD27 Datum

Figure 1.

